①

AFIT/GSO/OS/83D-1

AD-A141 136

DTIC FILE COPY

A COMPUTER MODEL FOR EVALUATION OF LAUNCH VEHICLE AND TARGET TRACKING ERROR ASSIGNMENTS FOR DIRECT ASCENT, DEEP SPACE ASAT SYSTEMS

THESIS

Richard C. Barclay
Captain, USAF
AFIT/GSO/OS/83D-1

DTIC
ELECTE
MAY 16 1984
S
A

Approved for public release; distribution unlimited

84 05 15 041

AFIT/GSO/OS/83D-1

A COMPUTER MODEL FOR EVALUATION OF LAUNCH VEHICLE AND TARGET TRACKING ERROR ASSIGNMENTS FOR DIRECT ASCENT, DEEP SPACE ASAT SYSTEMS

THESIS

Presented to the Faculty of the School of Engineering
of the Air Force Institute of Technology
Air University
In Partial Fulfillment of the
Requirements for the Degree of
Master of Science in Space Operations

Richard C. Barclay, B.S.A.E.
Captain, USAF

DTIC COPY [illegible]

December 1983

A-1

Approved for public release; distribution unlimited

Preface

This effort was suggested and sponsored by the Directorate of Space Systems, HQ SPACECOM. Their goal was a better understanding of how deep space tracking capabilities might impact the targeting of objects in deep space with a follow on Anti-satellite (ASAT) system. This was motivated in part by a recognition that our deep space tracking capabilities are not as good as those for low altitude satellites. Consequently, the possibility of targeting objects in deep space brought on concerns about how these tracking shortcomings would impact the system development. My purpose then was to develop a tool which could be applied to targeting situations to enable a first order evaluation of system implications for deep space ASAT.

I am indebted to many individuals and organizations for their support in this effort. First of all, I must thank my advisor, Lt. Col. Mark Mekaru for providing advice and guidance throughout, while still permitting me the latitude to develop the project in my own way. Dr. William Weisel provided invaluable assistance in setting up some of the key elements of logic in the model. Major Jim Lange was instrumental in evaluating the establishment of a technologically feasible range for ASAT sensor acquisition.

It is especially pleasing when people outside of the Institute and the sponsoring agency take enough interest in a project like this to expend some of their time and effort in support of it. I am indebted to Mr. Dave Whitcomb of the Aerospace Corporation for going out of his way to pass on some of his expertise in the area of inertial guidance systems and provide error data for some common systems. In the area of deep space tracking errors, Dr. Tony Pensa, Dr. Sid Sridrahan, and Mr. Bill Sinieu of MIT Lincoln Laboratory, and Capt. Glenn Hasegawa, formerly of Cheyenne Mountain's Deep Space shop, were extremely helpful.

Finally, and most importantly, to Barb, Tammy, and Matt, I express my gratitude for putting up with my reclusive habits throughout this experience. And, once again, my deepest love and thanks to my wife Barb whose professional typing skills turned all this ground work into the finished product before you now.

Richard C. Barclay

Table of Contents

Page

Preface ii

List of Figures vi

List of Tables vii

Abstract viii

I. Introduction 1

Problem 4
Scope and Assumptions 4
General Approach . . . .
Presentation 7

II. Astrodynamics, Error Generation, and Sensor Characteristics 8

Orbital Elements and Some Useful Astrodynamic Terms 9
The Gauss Problem (Subroutine INTCPT) 12
The Kepler Problem (Subroutine KEPLER) 16
Error Generation (Subroutine RNDMGN) 18
The Physics of Sensor Acquisition 19

III. Model Overview 25

The Model 25
The Program 29

IV. Model Applications 36

Introduction 36
The Inputs 36
Error Models 39
The Applications 44
Scenario One 51
Scenario Two 55
Scenario Three 55
Validation 56
Conceptual 57
Verification 57
Credibility 59
Confidence 60
Summary 61

Page

V. Conclusions and Recommendations. 63

Conclusions 63
Recommendations for Follow-On
Work. 63

Bibliography. 66

Appendix. 68

Vita. 80

List of Figures

Figure Page

2-1 Geocentric-Equatorial Coordinate System. 10

2-2 Basic Earth Orbit Geometry 11

2-3 Typical t vs. z Plot 15

2-4 Radial-Tangential-Normal Coordinate System 20

2-5 Similar Triangle Approximation for Delta V 23

3-1 Conceptual Model 26

3-2 Program ASAT's Role in Performance Tradeoffs 28

3-3 Computer Model 30

4-1 Comparison of Generic IGS Results to Actual Systems Data Results (Target A--4 Hour TOF). 40

4-2 Miss Distance vs. IGS Accuracy (Target A--4 Hour TOF) 46

4-3 Miss Distance as a Function of IGS Accuracy (Left) and Target Errors (Right) (Target A--3 Hour TOF). . . 47

4-4 Miss Distance as a Function of IGS Accuracy (Left) and Target Errors (Right) (Target B--3 Hour TOF). . . 48

4-5 Miss Distance as a Function of IGS Accuracy (Left) and Target Errors (Right) (Target C--3 Hour TOF). . . 49

4-6 Miss Distance as a Function of IGS Accuracy (Left) and Target Errors (Right) (Target D--3 Hour TOF). . . 50

4-7 Delta V vs. Acquisition Distance (IGS 1 and IGS 4, Various Target Errors, 3 Hour TOF) 52

4-8 Miss Distance as a Function of IGS Accuracy (Left) and Target Errors (Right) (Target A--4 Hour TOF). . . 53

3-2 Program ASAT's Role in Performance Tradeoffs 64

List of Tables

Table | Page

I. S/N for Selected Acquisition Distances 22

II. Sample Trajectory Inputs (Target A and C) 39

III. Injection Errors (1-sigma) for 3 IGS's with Burnout Velocity 35000 fps 41

IV. Scenario One 54

V. Scenario Two 55

VI. Scenario Three (IGS 4) 56

VII. Sample Results for Test of Sample Means (95% Confidence) 61

AFIT/GSO/OS/83D-1

ABSTRACT

An unclassified computer model was developed for first order evaluation of deep space Anti-satellite (ASAT) targeting error assignments. Two independent error sources are modeled. With deep space tracking accuracies on the order of kilometers, there is uncertainty in the exact target position. Errors introduced by the launch vehicle guidance system result in uncertainty in the exact position of the ASAT itself. Once the target is acquired by the ASAT sensor subsystem, the maneuver subsystem must then have the capability to make the necessary trajectory corrections to prevent a "miss."

The model assumes a direct ascent vehicle for which the user selects a trajectory by choosing the burnout and intercept position vectors, and a time of flight between them. Monte Carlo simulation is used to generate errors in burnout position and velocity, and intercept position from trivariate normal distributions scaled to user input standard deviations. This is repeated for 500 iterations, from which a mean miss distance and delta V required for trajectory correction can be determined, and used for further analysis.

Suggested applications are presented to show how the model results can be used as a measure of system performance for initial system tradeoff studies. Validation/verification and recommendations for further use are also provided. A program listing is included as an appendix.

A COMPUTER MODEL FOR EVALUATION OF LAUNCH VEHICLE AND TARGET TRACKING ERROR ASSIGNMENTS FOR DIRECT ASCENT, DEEP SPACE ASAT SYSTEMS

I. Introduction

Current Anti-satellite (ASAT) development efforts of both the United States and the Soviet Union have been limited to targets in relatively low earth orbit. The Soviet system is reportedly capable of reaching targets up to 600 to 1000 nautical miles (NM). The U.S. F-15 launched system is also limited to targets in low earth orbit. Both systems, however, could conceivably reach geosynchronous altitude (19,300 nautical miles or 35,500 kilometers) simply by launching them from expendable boosters capable of lifting such payloads to that altitude (12:244). In fact, Aviation Week and Space Technology has reported that a 1981 updated USAF ASAT requirement recognizes that higher geosynchronous type altitudes will be required of any follow-on or improved ASAT system (11:18).

It is aspects of this deep space ASAT targeting which are to be investigated here. Objects in deep space are those with an orbital period in excess of 225 minutes. The two most popular deep space orbital classes are the 24-hour geosynchronous and the highly inclined, highly elliptical, 12-hour Molniya. Molniya is used primarily by the Soviets, while both the United States and the Soviets have orbited satellites in the geosynchronous belt. Particularly essential as a first step toward targeting of objects in these orbits is an understanding of how launch vehicle guidance errors (resulting in some uncertainty of exact ASAT position) and target tracking errors (resulting in some uncertainty of exact target position) interrelate to produce errors which the ASAT acquisition sensor and maneuver subsystems must overcome if the ASAT is to acquire and intercept the target.

The real purpose of any guidance system is to minimize deviations from a nominal or desired trajectory. Most of these systems have well defined physical limitations. Even an inertial guidance system such as the Space Shuttle's can only sit on the pad for a limited amount of time before it must be realigned. This is because there is an error called "drift" that develops as a function of time, even when the vehicle is not moving with respect to the earth. There are ways to reduce these errors, such as improved gyro and accelerometer components, or use of a high order gravity model in the navigation computation (16). In fact, if it is possible to introduce information from an external source, such as the use of on-board doppler radar from ground beacons, these errors can be reduced to a virtually negligible amount (16). These improvements are not without a price. That price may be measured in dollars and cents or the political price of placing ground beacons in areas of the world where a continued presence is less than guaranteed. The point is, though, that guidance accuracy is a variable over which the developer/user has control.

Another variable is target tracking accuracy. That is the uncertainty of target position. Tracking accuracy on a particular target is basically dependent on what sensor(s) can view it, when and how much it was most recently "tracked", whether or not its orbit is one of a particularly predictable and stable nature, and, to some degree, what particular computational tools are used to predict the future position. The U.S. has typically done a h better job of tracking objects in lo th orbit than in deep space. Our Spacetrack network is capable of tracking low earth objects to an accuracy on the order of tens of meters or better. Objects in deep space are known, on the average, no better than 1-10 KM, and may be as bad as 200 KM (2). There are a significant number of objects in deep space which are categorized as "lost." These facts serve to point out the relative inadequacy of our deep space capability vis a vis near space (12:249; 9:83).

In the past, this tracking has been done primarily by Baker-Nunn cameras and the Millstone Hill radar operated by MIT Lincoln Laboratory in Massachusetts. Recent improvements to deep space surveillance capabilities include the Ground Based Electro-optical Deep Space Surveillance System (GEODSS), with 3 of 5 projected sites operational, and radar upgrades to existing systems at Kwajalein and Turkey. Even with these improvements, to date, 10 to 20 KM uncertainty is still considered about average (13:2). So it is, that target tracking accuracy is of much greater concern to a deep space ASAT system than it is to one in near space. One can either "design to" the current capability or insure we have a tracking system which is capable of providing the required accuracy, commensurate with spacecraft and ASAT characteristics, to permit successful intercept for all prospective targets.

ASAT characteristics, in particular sensor and maneuver capabilities, are the third major area of concern to this situation. Once the user defines the target list (thus defining tracking errors) and candidate guidance capabilities, it should be possible to determine what ASAT sensor and maneuver characteristics would be required to compensate for those errors and get the ASAT in position for intercept.

Problem

There is a lack of understanding about requirements for deep space ASAT targeting and the interrelationships among target tracking accuracy, launch vehicle accuracy, and ASAT sensor/maneuver capability.

Scope and Assumptions

The purpose of this thesis is to develop a computer program and analysis techniques which can be used as tools in a first order evaluation of a deep space ASAT system. The scenario considered is a direct ascent vehicle attacking satellites in geosynchronous equatorial and Molniya orbits. As previously stated, these are the two most popular deep space orbital classes. The trajectory is assumed to be a free flight from burnout (at approximately 100 NM altitude) to the point where the ASAT sensor can acquire the target and make the proper trajectory corrections to permit intercept. It should be noted that although this problem used the 100 NM burnout point as the starting point for error modeling, it could easily be done from some point later in the trajectory (a mid-course correction, for instance), as long as the position and velocity error characteristics can be described in a manner similar to those at burnout.

The astrodynamics involved are limited to 2-body approximations. The target does not maneuver while the ASAT is enroute. The actual search and acquisition of the target by the ASAT is not considered. A first order approximation of a technologically reasonable range from which a typical target can be seen is used to plot a range of delta V acquisition distances. (Delta V is the increment of velocity, representing an instantaneous "burn" by the propulsion system, required to change the magnitude and/or direction of the current velocity vector to one that is desired.) The intercept trajectories are assumed to be elliptical with a time of flight less than one orbital period, and the two input position vectors must be non-collinear.

General Approach

The computer program runs a user selected intercept and outputs an expected miss distance and delta V required for intercept from several acquisition distances. The intercept subroutine, which is used to establish a "nominal" trajectory against which the "error-induced" trajectories can be compared, borrows a "Gauss problem" algorithm from Fundamentals of Astrodynamics by Bate, Mueller and White (1:234). The "Gauss problem" determines an orbit given two position vectors and a time of flight between the two. It was used initially to help develop a hypothetical intercept mission. Also from Bate, Mueller and White, is the KEPLER subroutine which outputs a position and velocity vector when given initial position and velocity vectors and a time of flight (1:203). The error generation subroutine (called RNDMGN in the program) randomly generates errors from a standard normal distribution in each component of the Radial-Tangential-Normal coordinate system, which are then "scaled" to the input error characteristics. These scaled errors are then converted to the Geocentric-Equatorial coordinate system.

The top level logic using these subroutines is as follows: (1) compute a nominal intercept trajectory with subroutine INTCPT; (2) compute a new initial position and velocity and "actual" target position based on the random errors generated in RNDMGN; (3) use subroutine KEPLER to predict the "error-induced" interceptor position at the given time of flight; (4) compute "miss distance" (the difference between the KEPLER predicted interceptor position and the "actual" target position); (5) compute delta V's vs acquisition distance using a similar triangle approximation (both trajectories approximate straight lines at these distances). Steps (2)-(5) are repeated 500 times to establish averages for miss distance and delta V.

Mr. Dave Whitcomb at the Aerospace Corporation was kind enough to provide some data on some of our most commonly used (albeit somewhat aged) inertial guidance systems. The Air Force Space Command and MIT Lincoln Laboratory provided information about different classes of target tracking errors, and class notes from Physics 6.21 (taught by Maj. Jim Lange at AFIT) were used to determine a range of technologically feasible sensor acquisition distances. This information provides a starting point for examining a hypothetical deep space ASAT system against hypothetical targets.

This examination includes some initial data runs to insure the model is at steady state. Steady state conditions were determined to be that number of iterations where the mean miss distance changed less than 5% with additional iterations. As many as 2500 iterations of the error generation portion of the model were attempted to insure that 500 was sufficient. Another sequence of runs investigated the effect of varying time of flight on a particular target, and the difference between a Molniya and a geosynchronous target. A "generic" inertial guidance system was created and used to determine the effects of improved guidance accuracy for different target classes. This generic system was spherically symmetric in error characteristics and produced results very similar to that of the actual system data provided by Aerospace Corporation.

Presentation

Chapter Two addresses the technical aspects of the orbital mechanics, random error generation, and sensor physics used in the model. Chapter Three describes the model and the computer program. Chapter Four deals with applications, how the model was used, suggested future uses, and model validation. Chapter Five presents conclusions and recommendations based on the particular uses described here.

II. Astrodynamics, Error Generation, and Sensor Characteristics

The astrodynamics of this problem involves two very famous orbital mechanics problems. The "Gauss problem", so called because Carl Fredrich Gauss proposed its initial formulation in 1801, is one of determining an orbit based on two positions and a time of flight. Bate refers to it as "the most brilliant chapter in the history of orbit determination" (1:227). The "Kepler problem" is one of predicting the future position and velocity of a satellite based on an initial position and velocity and a time of flight. The Keystone of this thesis is error generation, which assumes some knowledge of launch vehicle and target error characteristics on the part of the user. That is, that guidance system and target position error characteristics can be described with respect to a coordinate system centered on the vehicle/target itself. These characteristics may then be used to "scale" the Monte Carlo generated errors to the input parameters. The third player in the scenario is the ASAT itself and its sensor and maneuver subsystem capabilities to overcome the previously described errors. No attempt will be made to "design" these subsystems. Some first order calculations will be done to determine a technologically feasible range of sensor acquisition distances from which energy requirements for maneuver to intercept (delta V) can be estimated. The average miss distance and its translation to delta V requirements are the basic units of measurement to be used in evaluations performed with this model.

This chapter will include an overview of the elements used to describe an orbit and some terms which will be important, the highlights of the two astrodynamic algorithms, a description of the error generation in

Subroutine RNDMGN, and the physics of a feasible sensor for the ASAT. This is not meant to be a rigorous development, but will provide insight into the theory involved in the model and lead to the discussion of the actual program in Chapter III. (All astro developments are drawn from Fundamentals of Astrodynamics by Bate, Mueller and White, henceforth referred to as "Bate".)

Orbital Elements and Some Useful Astrodynamic Terms

At the heart of this development is the Geocentric-equatorial coordinate system (see Figure 2-1). It is a right-handed system with the earth's center at its origin. The X-axis (represented by the I unit vector) points toward the vernal equinox, and the Z-axis (represented by the K unit vector) points toward the north pole. Note that the system is nonrotating with respect to the stars, with the earth rotating relative to the frame.

The intercept orbits in this effort are elliptical (as opposed to parabolic or hyperbolic), and the basic geometry of an elliptical orbit is shown in Figure 2-2. Some of the key items to note are as follows:

1. The earth is at one focus of the ellipse
2. The point of closest approach to earth is called perigee
3. The point at which the object is farthest from earth is apogee
4. The major axis is a line joining apogee and perigee. The semi-major axis is more commonly referred to in describing the shape of an orbit and, as the name implies, its length is half that of the major axis and is denoted by the letter "a".
5. The angle between two position vectors is denoted as $\Delta\nu$ in this problem. The angle ν_0 is the angle from perigee to the orbiting

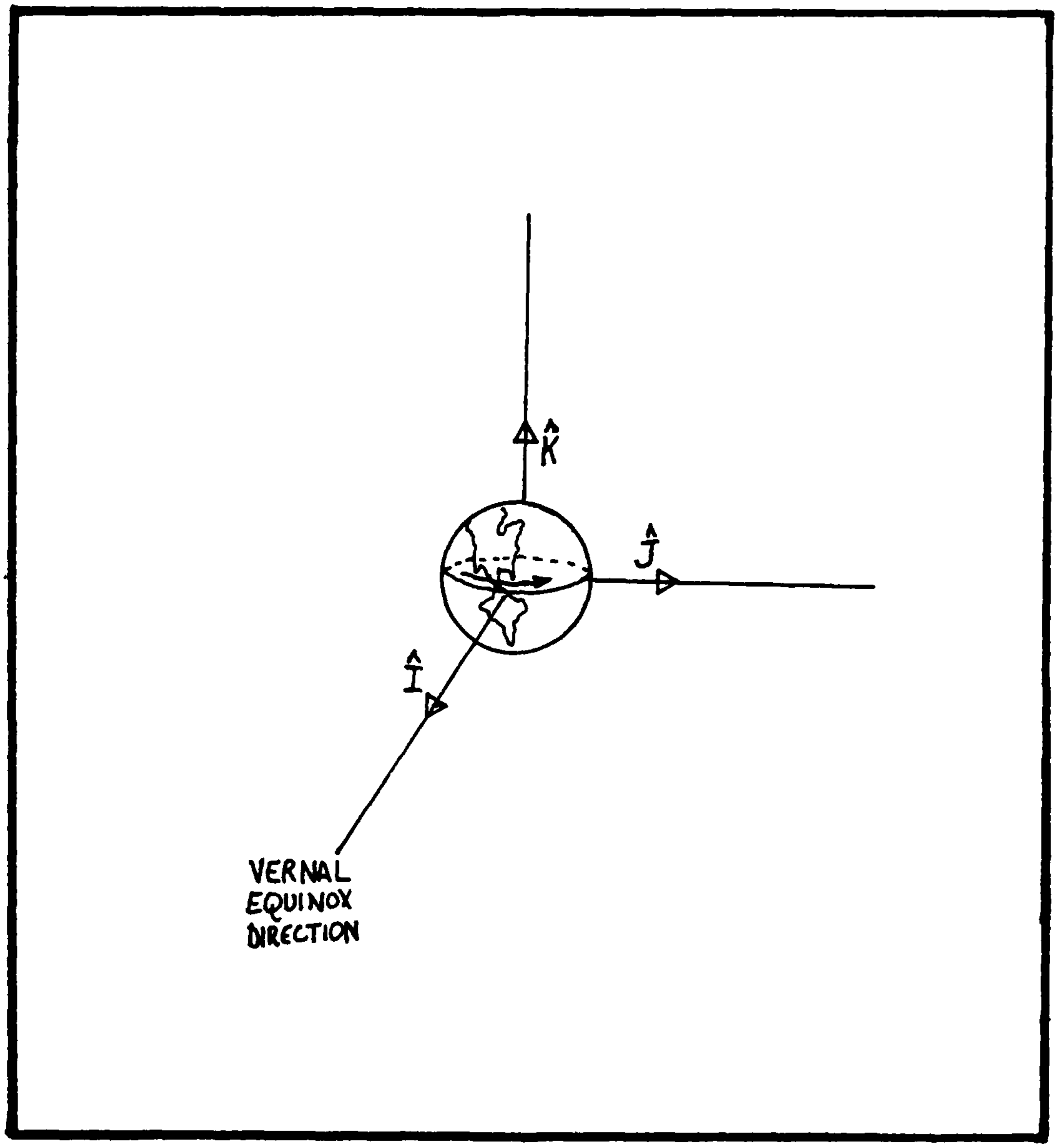

Figure 2-1. Geocentric-Equatorial Coordinate System

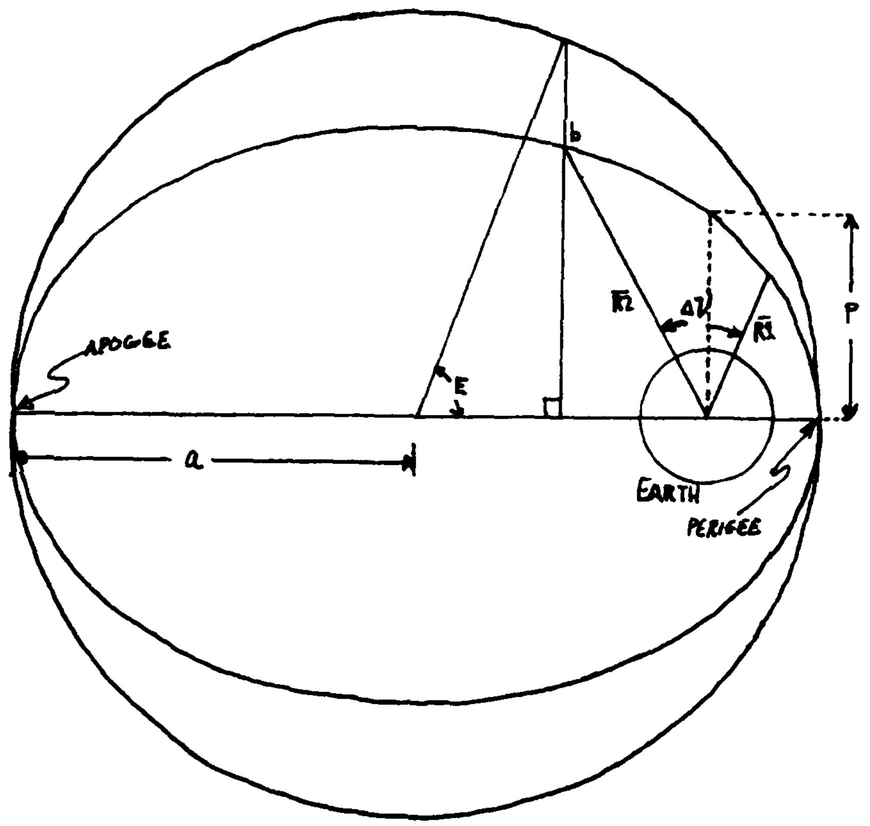

Figure 2-2. Basic Earth Orbit Geometry

object measured in the direction of motion, referred to as the "true anomaly." The magnitude of the position vector when the true anomaly is 90 degrees is referred to as the "semi-latus rectum", denoted by the letter "p".

6. The eccentric anomaly is the angle "E" shown in figure 2-2. It is formed by circumscribing a circle of radius "a" about the ellipse and drawing a line perpendicular to the major axis through position "b" on the ellipse to the circle.

The Gauss Problem (Subroutine INTCPT)

The Gauss problem computes velocity vectors at two positions in an orbit when given those two position vectors, $\overline{R1}$ and $\overline{R2}$, and the time of flight (and direction of motion) between them. The basic idea is to guess a value of the change in eccentric anomaly (represented by universal variables) and, by using the time of flight equation, iterate to the correct value, from which the desired output ($\overline{V1}$ and $\overline{V2}$) can be computed. The following is the algorithm as presented in section 5.3 of Bate (further explanation of certain steps, variables, and functions used will follow):

1. From $\overline{R1}$, $\overline{R2}$, and the direction of motion, evaluate the constant, A, using:

$$A = \frac{(R1 \times R2)^{\frac{1}{2}} \sin \Delta\nu}{(1- \cos \Delta\nu)^{\frac{1}{2}}} \tag{1}$$

2. Pick a trial value for z.

3. Evaluate the functions S and C for the selected value of z using:

$$C(z) = \frac{1- \cos (z)^{\frac{1}{2}}}{z} \tag{2}$$

$$S(z) = \frac{(z)^{\frac{1}{2}} - \sin (z)^{\frac{1}{2}}}{(z^3)^{\frac{1}{2}}} \tag{3}$$

4. Determine the auxiliary variable y, using:

$$y = R1 + R2 - A\,\frac{(1- zS)}{(C)^{\frac{1}{2}}} \qquad (4)$$

5. Determine x from:

$$x = \left(\frac{y}{C}\right)^{\frac{1}{2}} \qquad (5)$$

6. Check the trial value of z by computing time of flight using:

$$(\mu)^{\frac{1}{2}}t = x^{3}S + A(y)^{\frac{1}{2}} \qquad (6)$$

($\mu = 1$ since all computations are in canonical units.)

Compare the computed time of flight to the desired (input). Iterate steps 2 through 6 until the computed time matches the desired, within acceptable tolerance. (Exact iteration scheme used will be explained in Chapter III.)

7. When convergence is complete, compute f, g and $\dot{g}$ using:

$$f = 1 + \frac{y}{R1} \qquad (7)$$

$$g = A\ (y/\mu)^{\frac{1}{2}} \qquad (8)$$

$$\dot{g} = 1- y/R2 \qquad (9)$$

8. Compute $\overline{V1}$ and $\overline{V2}$ using:

$$\overline{V1} = \frac{\overline{R2} - (f)\ \overline{R1}}{g} \qquad (10)$$

$$\overline{V2} = \frac{(\dot{g})\ \overline{R2} - \overline{R1}}{g} \qquad (11)$$

This algorithm makes use of the universal variables x and z, as formulated in Chapter 4 in Bate. The variable x is defined as:

$$\dot{x} = (\mu)^{\frac{1}{2}}/r \qquad (12)$$

and the z variable as:

$$z = x^{2}/a \qquad (13)$$

The introduction of such variables eliminates some computational inadequacies for certain orbit geometries and permits development of a single time of flight equation applicable to all conic orbits (1:191). They are physically related to the eccentric anomaly (E) and, therefore, to the specific orbit itself, by the following relations:

$$x = a^{\frac{1}{2}} (E - E_0) \tag{14}$$

$$z = (E - E_0)^2 \tag{15}$$

Of particular importance to this development is the behavior of z as a function of time. This relationship is shown in Figure 2-3. With the assumption that trajectories under consideration will all be ellipses whose associated times of flight will be less than one period, Figure 2-3 shows that we can iterate on this function between two distinct end points (0 and $(2\pi)^2$). This fact is exploited in the program and will be revisited in Chapter III.

Step 1 in the algorithm calls for a direction of motion for the trajectory. This is required because for every two position vectors (assuming they are not collinear) and time of flight, the vehicle could travel two possible routes between the two vectors. In one route the angle between the two position vectors ($\Delta\nu$) is less than 180 degrees. It is called the "short way." The other route occurs when $\Delta\nu$ is greater than 180 degrees. Choosing the direction of motion makes it possible to determine a unique orbit based on the given parameters. The collinear cases ($\Delta\nu$ equal to 180 or 0) require more than the generalized treatment here and are not considered.

The A term in step 1 is simply a constant determined by the inputs which simplifies a number of equations in the algorithm. The C and S terms in step 3 are functions of z which are required in the

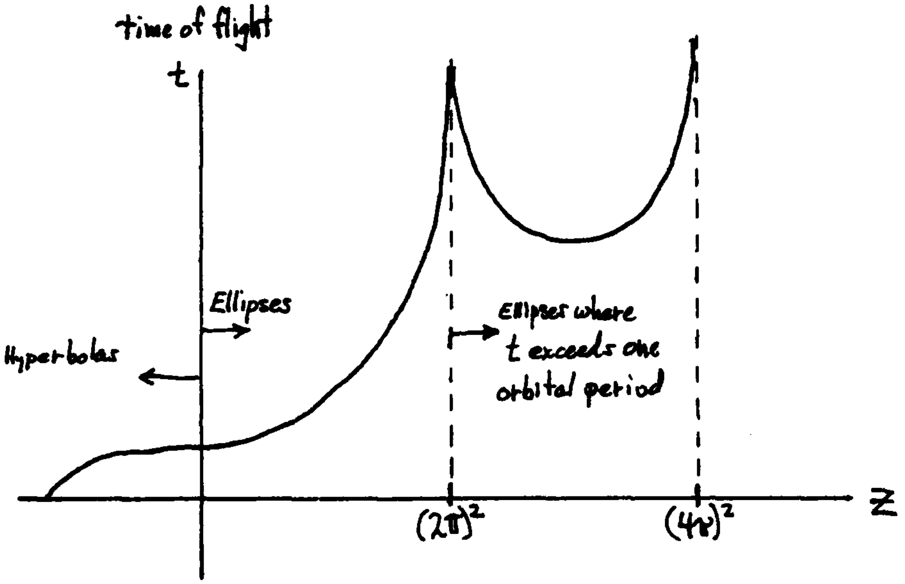

Figure 2-3. Typical t vs. z Plot
(1:235)

development of the time of flight expression (steps 4, 5, and 6).

The transition from the universal variables to the desired output ($\overline{V1}$ and $\overline{V2}$) is accomplished by application of the f and g expressions. These expressions can be developed because Keplerian motion is confined to a plane. This means that the vectors $\overline{R1}$, $\overline{R2}$, $\overline{V1}$, and $\overline{V2}$ are all coplanar. Making use of a fundamental theorem that if three vectors are coplanar, and two are not collinear, then the third can be expressed as a linear combination of the first two. Therefore, $\overline{R2}$ and $\overline{V2}$ can be expressed as follows:

$$\overline{R2} = (f)\overline{R1} + (g)\overline{V1} \qquad (16)$$

$$\overline{V2} = (\dot{f})\overline{R1} + (\dot{g})\overline{V1} \qquad (17)$$

It can be shown (Bate Section 4.4.3) that the f and g expressions are the following:

$$f = 1 - \frac{x^2 C}{R1} \qquad (18)$$

$$g = t - \frac{x^3 S}{(\mu)^{\frac{1}{2}}} \qquad (19)$$

$$\dot{f} = \frac{(\mu)^{\frac{1}{2}} x}{(R1)(R2)} (zS-1) \qquad (20)$$

$$\dot{g} = 1 - \frac{x^2 C}{R2} \qquad (21)$$

These expressions are then simplified by the use of the constant A and the auxiliary variable y to those shown in step 7. They are then used in the equations in step 8 to achieve the desired output ($\overline{V1}$ and $\overline{V2}$).

The Kepler Problem (Subroutine KEPLER)

The Kepler Problem predicts the position and velocity vectors after some given time of flight has elapsed, when given the initial position and velocity vectors. This algorithm also makes use of the universal variables, f and g expressions, and C and S functions discussed in the previous section. The basic logic of this algorithm is to guess a value of x, use z, C, and S to compute the time of flight, iterate until the computed time of flight equals the desired value, and use that x, C and S in the f and g expressions to compute $\overline{R2}$ and $\overline{V2}$.

The actual algorithm is:

1. Compute a using:

$$a = -\frac{\mu}{(V1)^2 - \frac{2\mu}{R1}} \tag{22}$$

2. Pick a trial value for x using:

$$x = \frac{(\mu)^{\frac{1}{2}}(t-t_0)}{a} \tag{23}$$

3. Determine z, C, and S using:

$$z = \frac{x^2}{a} \tag{13}$$

$$C(z) = \frac{1 - \cos(z)^{\frac{1}{2}}}{z} \tag{2}$$

$$S(z) = \frac{(z)^{\frac{1}{2}} - \sin(z)^{\frac{1}{2}}}{(z^3)^{\frac{1}{2}}} \tag{3}$$

4. Check the trial value of x by computing time of flight:

$$(\mu)^{\frac{1}{2}}t = \frac{\overline{R1}\cdot\overline{V1}}{(\mu)^{\frac{1}{2}}}\, x^2 C + (1 + \frac{R1}{a})\, x^3 S + (R1)x \tag{24}$$

Compare the computed time of flight to the desired (input). Repeat steps 2 thru 4 until the computed time matches the desired time within acceptable tolerance. (Exact iteration scheme will be explained in Chapter III.)

5. Compute f and g using:

$$f = 1 - \frac{x^2 C}{R1} \qquad (18)$$

$$g = t - \frac{x^3 S}{(\mu)^{\frac{1}{2}}} \qquad (19)$$

6. Determine $\overline{R2}$ from:

$$\overline{R2} = (f)\overline{R1} + (g)\overline{V1} \qquad (16)$$

7. Evaluate $\dot{f}$ and $\dot{g}$ using:

$$\dot{f} = \frac{\mu^{\frac{1}{2}} x}{(R1)(R2)}(zS - 1) \qquad (20)$$

$$\dot{g} = 1 - \frac{x^2 C}{R2} \qquad (21)$$

8. Compute $\overline{V2}$ from:

$$\overline{V2} = (\dot{f})\overline{R1} + (\dot{g})\overline{V1} \qquad (17)$$

The universal variables and f and g expressions are the same ones described in the Gauss algorithm. No further explanation of them is required. Specific programming techniques and choices will be explained in more detail in Chapter III.

<u>Error Generation (Subroutine RNDMGN)</u>

In this model errors are modeled by trivariate normal distributions in a Radial-Tangential-Normal (R-T-N) coordinate system whose origin is centered at the subject of errors (vehicle/target). The R-T-N system was chosen because that is the usual way error characteristics of inertial guidance systems are described (16). It also seemed well suited for describing the target errors which are represented by a standard deviation (1-σ) predominantly "along the trajectory" (13:5). "Along the trajectory" is the Tangential direction in the cases considered here (geosynchronous equatorial being circular, and Molniya engagements limited to apogee).

An example of this coordinate system and its relation to the geocentric-equatorial system is shown in Figure 2-4. As stated, the origin is the vehicle itself. The radial unit vector is determined by the vehicle position vector, the normal is perpendicular to the plane of the orbit and can be found by taking the cross product of the position and velocity vectors. The tangential direction is found by crossing the normal and the radial.

The actual generation of the errors is accomplished by drawing three random numbers from a standard normal distribution (one for each R-T-N direction), scaling the values by multiplying each by its respective input error characteristic, and then converting these R-T-N error components to their respective geocentric-equatorial components. This Subroutine is called three times for each iteration, once for target position error and twice for ASAT position and velocity errors at burnout.

The Physics of Sensor Acquisition

One of the outputs of this model is a first order approximation of required acquisition distance/delta V combinations, given a target list and guidance parameters, for an ASAT to get in position for target kill. Therefore, it is necessary to make some estimation of what distances are technologically feasible for acquisition of the target. The calculations that follow will establish that feasible range. Once again, no attempt is made here to model the terminal intercept phase or the search procedure and probability of acquisition. Acquisition is assumed with sufficient signal-to-noise ratio. Discrimination of the target from the stellar

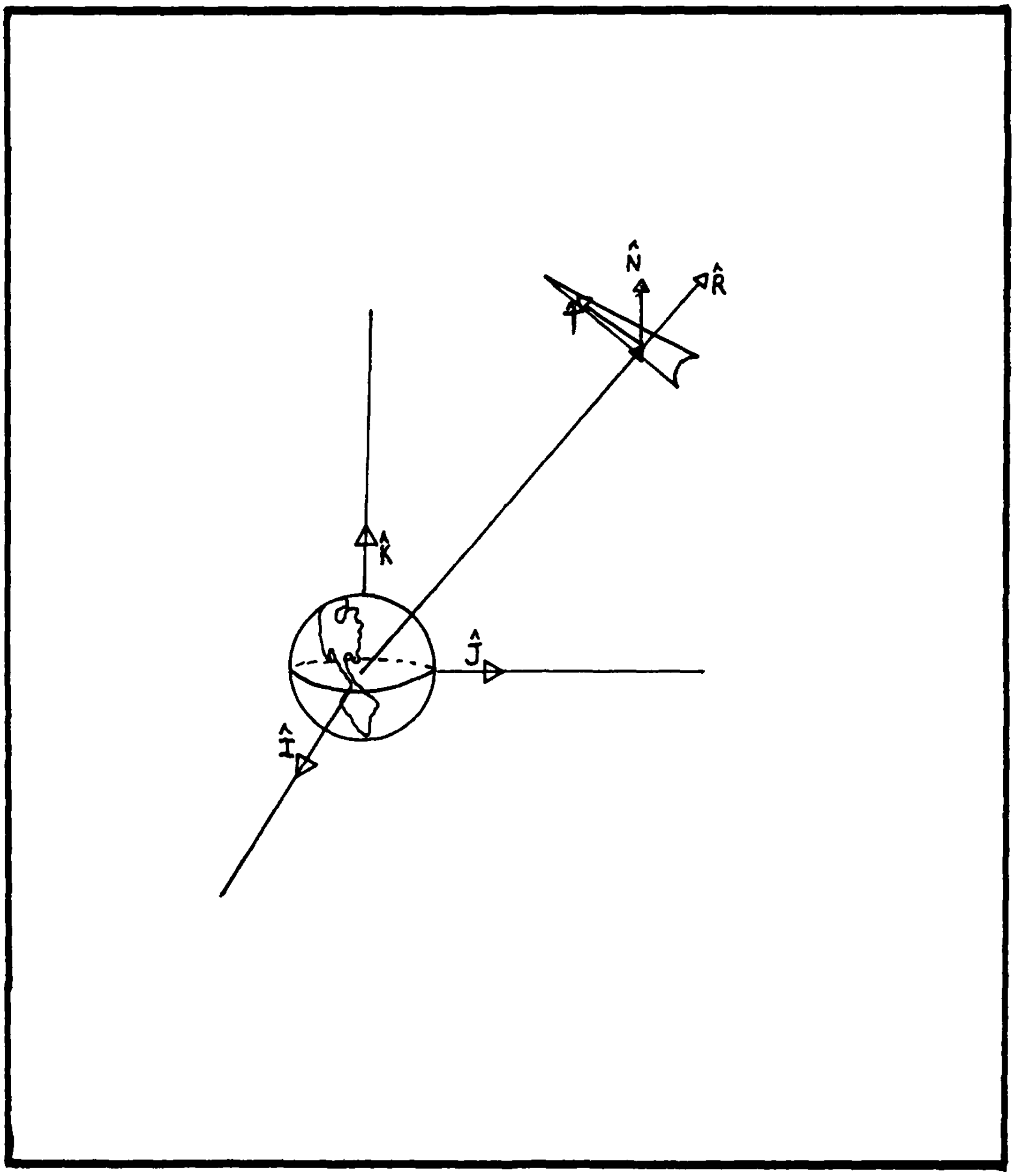

Figure 2-4. Radial-Tangential-Normal Coordinate System

background is achieved by sensing target motion with respect to that background. Once acquisition and discrimination are accomplished, the delta V maneuver is applied to get the vehicle to the point where minimal terminal maneuvers are necessary. The "acquisition distance" referenced here is that distance where both acquisition and discrimination have been achieved.

To determine what ranges will provide sufficient signal-to-noise, the following is taken largely from a development of a spaceborne sensor for tracking objects in space, as presented in Physics 6.21, an AFIT course in Electro-optical Space Systems Technology. The target is assumed to be a perfect 300^{0} K black-body, Lambertian source, with an emitting area of one square meter. This is the accepted "standard target" in the infrared community. The ASAT sensor could be a linear array of 200 mercury-cadmium-telluride detectors. Specific sensor parameters are:

1. Each individual detector has a diameter of one millimeter.
2. Total field of view (half angle) is 11.3 degrees.
3. Focal length is one meter.
4. Quantum efficiency is 0.25.
5. Spectral bandpass is 8-9 microns in the long wavelength infrared.
6. Diameter of the collecting optics is 0.5 meter.
7. Scan of the field of view is made by a rotation of the linear array once every second.
8. Dwell time (the integration time of the sensors) is 1.6×10^{-4} seconds.
9. Detector, housing, baffles, and collecting mirror are cooled to 77^{0} K by liquid nitrogen.

The objective is to determine if the signal-to-noise (S/N) ratio is high enough to permit acquisition and discrimination of the target from the background. A S/N of 10 will be considered sufficient for these purposes (7). The Infrared Handbook states that the largest spectral radiance value due to celestial objects in the sky at 11 microns is 3.5×10^{-7} W/m^2 ster μm (6:3-32). This assumes looking "away" from the earth, sun, and moon, with simple star background. Table I shows the results of S/N calculations for this background limited case (using only photon noise) with a standard target. Note that acquisition distances as great as 2000 KM are possible with these approximations before the limit (S/N = 10) is approached.

Table 1

S/N for Selected Acquisition Distances

Distance (KM)	S/N
250	233
500	120
1000	58
1500	37
2000	28

With the miss distance computed, based on the new error-induced interceptor trajectory and target tracking errors, the computation of delta V requirements for the feasible acquisition range remains. This is achieved by approximating the trajectories as straight lines. This approximation is acceptable for such small segments of trajectories with such large radii of curvature. As shown in Figure 2-5, application of similar triangles permits calculation of delta V. The velocity (V)

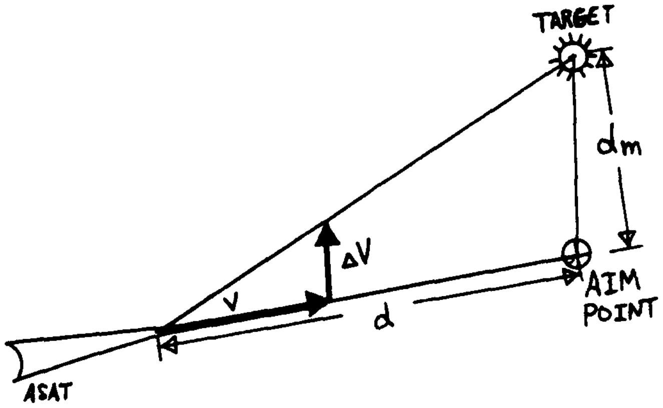

Figure 2-5. Similar Triangle Approximation for Delta V

computed by KEPLER is directed at the aim point which is the new R2 from KEPLER. The target is offset from the aim point by the "miss distance" computed in the program (dm). The distance "d" is the acquisition distance. The objective is to change the direction of the velocity vector so that the aim point and the target coincide. By similar triangles, one can see that

$$\frac{d_m}{d} = \frac{\Delta V}{V} \tag{25}$$

and, solving for delta V

$$\Delta V = \frac{d_m V}{d} \tag{26}$$

This is done for acquisition distances of 250, 500, 1000, and 2000 KM in the program. The next Chapter will present more details about the model and specific programming decisions which were made.

III. Model Overview

This chapter will provide more details about the model formulation and the computer program development.

The Model

A conceptual model is shown in Figure 3-1. It shows an intercept trajectory between two position vectors which is uniquely defined when a time of flight and direction of flight are chosen. This uniquely determined trajectory is what has heretofore been called the nominal trajectory. The first position vector ($\overline{R1}$) is at the point where the interceptor begins free flight toward the projected target position, which is the second position vector ($\overline{R2}$).

What makes this problem interesting to study are the uncertainties in both ASAT and target positions as they approach intercept. The ASAT is launched from the earth's surface and is carried to the burnout point ($\overline{R1}$) by the launch vehicle. This launch vehicle's guidance system is not perfect and there results some uncertainty in both position and velocity at $\overline{R1}$. These position and velocity errors created by the launch vehicle guidance system propagate for the duration of the free flight portion of the mission. These result in the interceptor being off the nominal trajectory when it begins searching for the target. In addition, the target itself is not exactly where it was projected to be. The position errors are caused by tracking inaccuracies. So there are two independent sources of errors which, if uncorrected, will result in a miss distance between the ASAT and target. To overcome these errors the ASAT acquisition subsystem must acquire the target and make a propulsive "burn" to correct

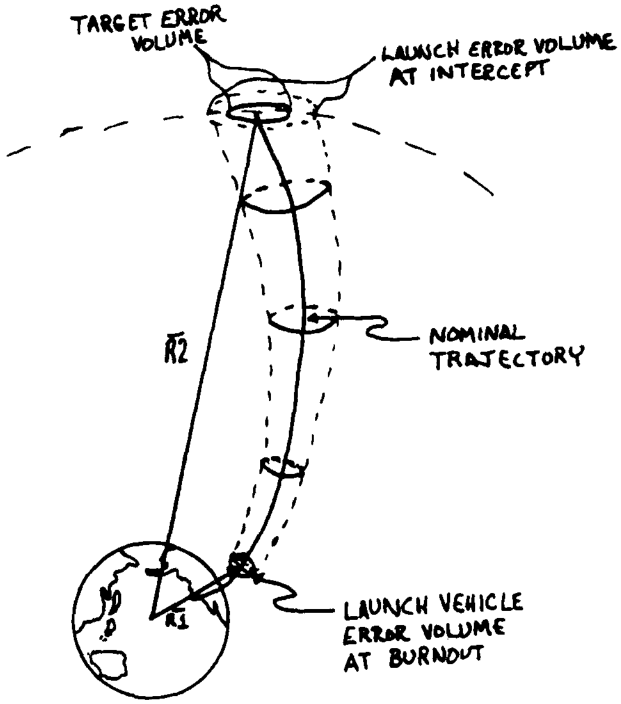
TARGET ERROR VOLUME
LAUNCH ERROR VOLUME AT INTERCEPT
$\bar{R}2$
NOMINAL TRAJECTORY
R1
LAUNCH VEHICLE ERROR VOLUME AT BURNOUT

Figure 3-1. Conceptual Model

the ASAT's flight path.

These errors can be statistically characterized and, it is possible to estimate how much energy (delta V) is required to make the necessary course correction. Information from experts indicated that both guidance errors and target tracking errors could be modeled by use of trivariate normal distributions in the R-T-N coordinate system (13:5). The error parameters input for the program are the 1-sigma values in each of the R-T-N directions. These are used to scale random numbers generated from a standard normal distribution. The subroutine RNDMGN is used to do this and then transform the R-T-N errors to the geocentric-equatorial system so they may be added directly to the respective vector. This is done to $\overline{R1}$ and $\overline{V1}$, which are then used to predict a new error-induced trajectory. It also operates on the target position, which then provides an actual target position at intercept. The magnitude of the vector between the new $\overline{R2}$ from KEPLER and the actual target position at intercept is the miss distance. Then by use of the similar triangle approximation explained in Chapter II, the delta V versus acquisition distances can be computed.

Figure 3-2 shows the author's concept of how this program might be used in an evaluation of a deep space ASAT system early in the system life cycle. It is intended that, from the defined operational need, a system operational concept would evolve over time. This would enable the user to define a target list from which target position errors could be defined. Candidate launch vehicle guidance system(s) with their characteristic errors, and ASAT subsystem characteristics (sensor, delta V and weight) can then be evaluated with Program ASAT by examining specific trajectories most appropriate for this operational concept. From those

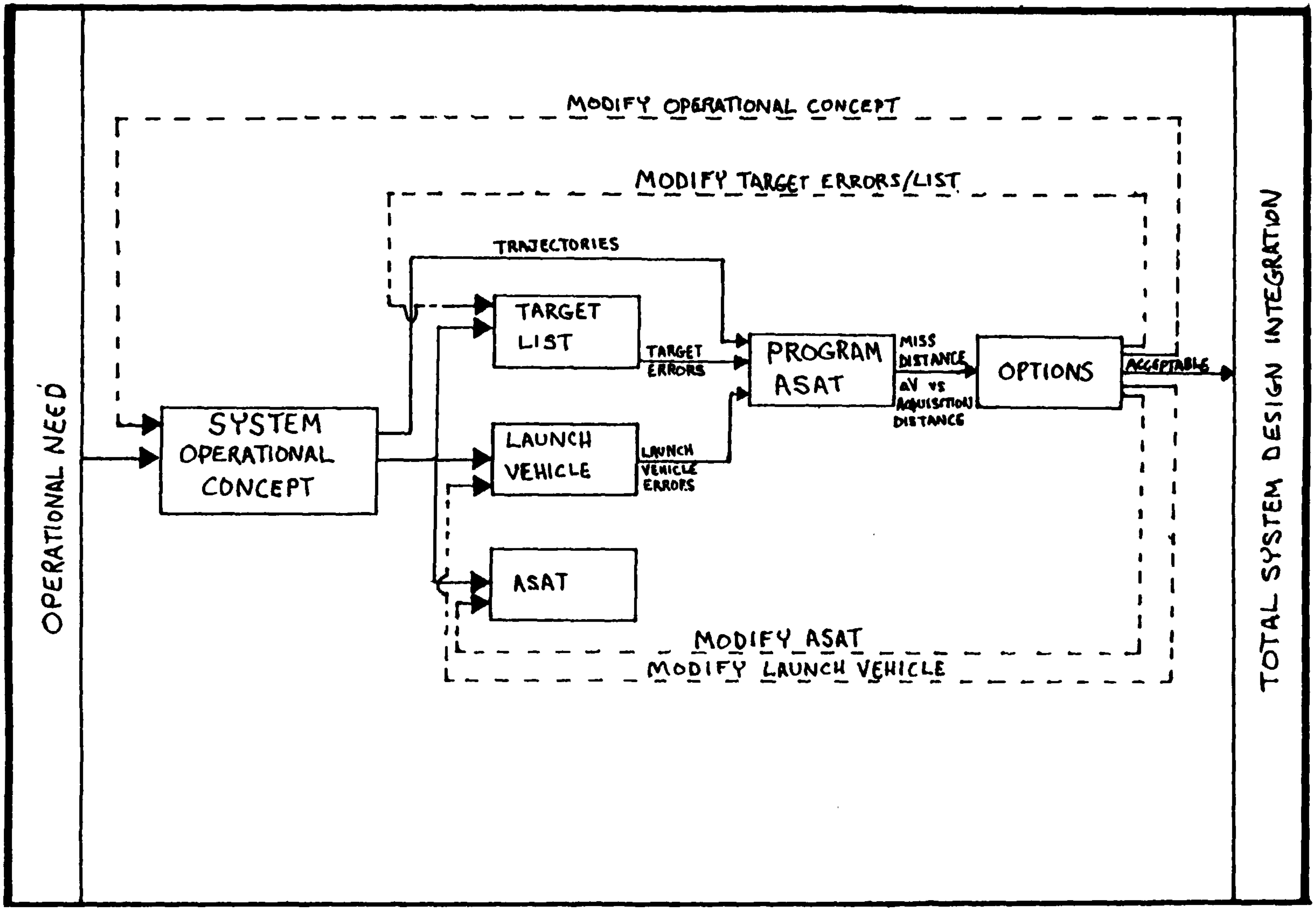

Figure 3-2. Program ASAT's Role in Performance Tradeoffs

results, the user can get a first order approximation of how the two sources of errors interact based on those systems parameters and what ASAT sensor/delta V tradeoffs are possible.

The analysis and interpretation of the results can then be used to refine the parameters used as Program inputs based on specifying one or more subsystem characteristics or perhaps altering the operational concept. It is possible to determine what guidance characteristics are required if constrained by ASAT sensor/delta V combination and target tracking. It is also possible to determine a delta V required based on the other parameters. This can then be converted to propellant mass required to insure the selected launch vehicle can lift the ASAT and propellants to the required targets. Another approach deals with examining relative payoffs, as measured by delta V, which can be achieved by improved tracking capability or guidance accuracy. Applications will be addressed in detail in Chapter IV. At this point it is appropriate to "walk through" the program to provide a better understanding of its structure and the reasoning for that structure.

The Program

Program ASAT was written in FORTRAN 5, and developed using a Control Data Corporation (CDC) Cyber computer. Figure 3-3 shows the top level logic of the program. There are three major subroutines involved in the scheme: INTCPT, KEPLER, and RNDMGN. The user inputs are:

1. $\overline{R1}$ - the position vector at orbital insertion (burnout) or the beginning of free flight. This is input in earth based canonical units as are all subsequent inputs. The three geocentric equatorial components must be entered in sequence, I, J, and K (variable names are R1I, R1J, and R1K in the program).

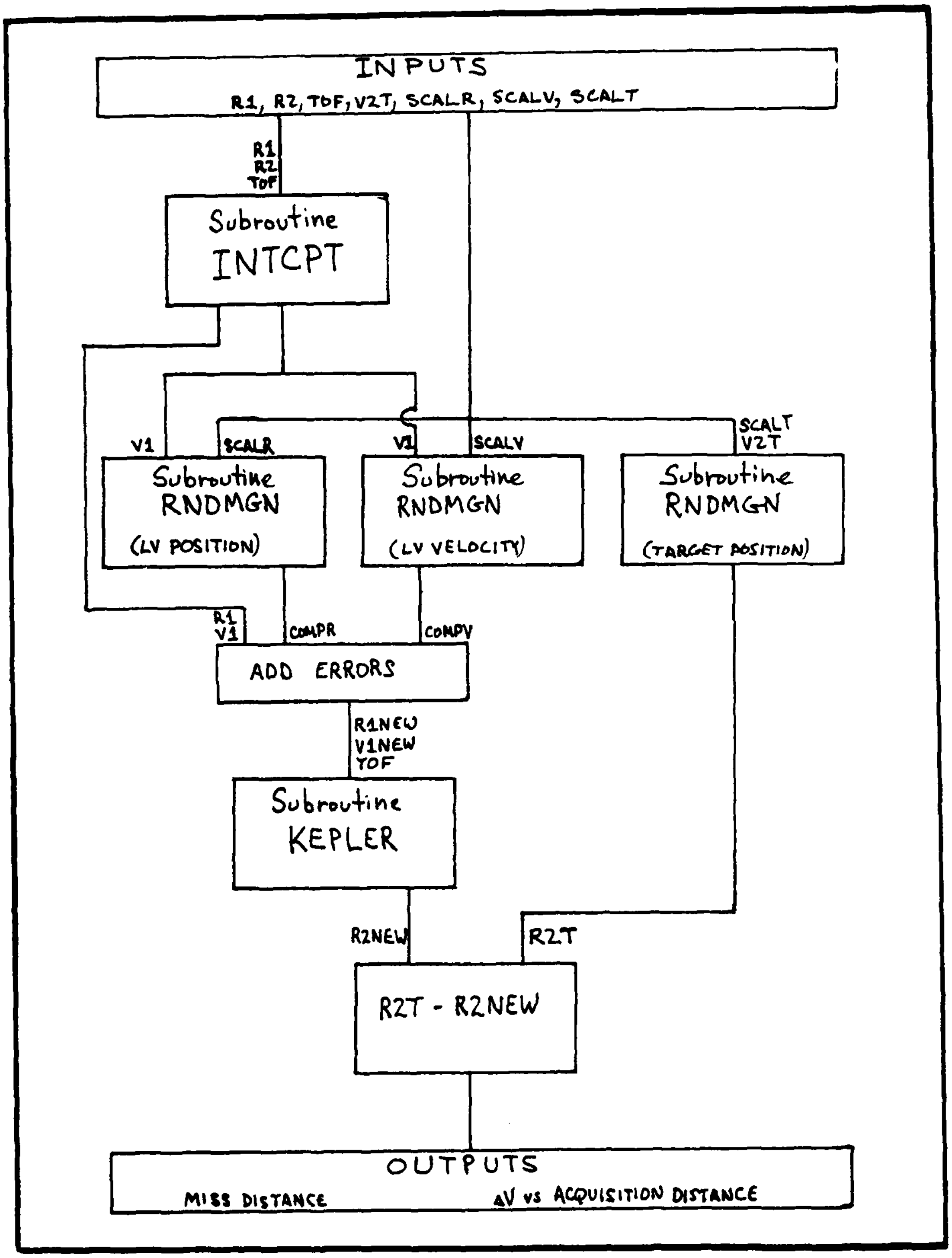

Figure 3-3. Computer Model

2. $\overline{R2}$ - the predicted position vector for intercept (I, J, K components whose variable names are R2I, R2J, and R2K).

3. Time of Flight - the time from $\overline{R1}$ (burnout) to intercept (variable name - TOF).

4. Position error parameters of launch vehicle guidance at burnout (1-σ values for R, T, N components whose variable names are SCALRR, SCALRT, and SCALRN).

5. Velocity error parameters of launch vehicle guidance at burnout (1-σ values for R, T, N components whose variable names are SCALVR, SCALVT, and SCALVN).

6. Target tracking error parameters (1-σ values for R, T, N components whose variable names are SCALTR, SCALTT, and SCALTN).

7. Target velocity vector at intercept (I, J, K components whose variable names are V2IT, V2JT, and V2KT).

Subroutine INTCPT uses $\overline{R1}$, $\overline{R2}$, and TOF to compute a nominal intercept trajectory and prints out the velocity vectors ($\overline{V1}$ and $\overline{V2}$) associated with the two positions. Trajectories were limited to the "short way" ($\Delta\nu$ less than 180 degrees) for this analysis. This approach would limit the vehicle's exposure to detection on its route. Should the user desire to consider the "long way", the program could be modified by adding a line in Subroutine INTCPT just after the computation of the variable DELNU, to replace it with its complement ("DELNU=2*PI-DELNU").

In the same subroutine, a bisection technique is used to iterate to the proper value of z, the universal variable described in Chapter II. Because of the transcedental nature of the equations in this scheme, numerical iteration is required. Bisection involves defining a specific interval in which the variable of interest is located. A check is made of the value of the function at the midpoint of this interval. If that value is larger than desired, the midpoint becomes the new upper limit on the interval, and if it is smaller, the midpoint becomes the new lower limit. Each iteration halves the interval and convergence is guaranteed (15:241).

The bisection method was chosen because in this case the z variable is known to occur on a very well-defined interval (0 to $(2\pi)^2$ as shown in figure 2-3). This is because of the trajectory assumptions discussed in Chapters I and II. It is, admittedly, not the most efficient iteration scheme, but it does offer the advantage of guaranteed convergence to within a specified interval when the initial interval is known. That "specified" convergence interval is dependent only on the size of the initial interval and the number of iterations (14:95). In this program there are 30 iterations with an initial interval of 39.478418, so convergence is within 3.7×10^{-8}. This is more than sufficient for the analysis performed, but it is also another place the user could, simply by changing the number of iterations, alter the program to specific needs (more or less accuracv, more or less computer time).

At this point, subroutine RNDMGN is used to generate errors in $\overline{R1}$, $\overline{V1}$, and target position ($\overline{R2}$) at intercept. Since the Cyber random number generator gets its random numbers from a uniform distribution, an application of the Central Limit Theorem is used to convert these random numbers to a standard normal distribution (10:362). This is done by summing 12 numbers from the uniform distribution and subtracting 6 from the sum to generate each standard normal number. According to Shannon, this method does not do well in the tails of the normal distribution beyond 2-σ. A more complex technique, also presented in Shannon, designed to overcome this weakness, did not appreciably affect the results in some initial baseline runs, so it was decided to go with simplicity. Three standard normal random numbers are drawn, one for each R-T-N component. Each is then scaled by multiplying by the input error parameter, which is a 1-σ value. These errors are then converted to the geocentric equatorial system by the cross products described in Chapter II. The components may then be added directly to the appropriate vector ($\overline{R1}$, $\overline{V1}$, and $\overline{R2}$) to simulate errors.

KEPLER then uses the new $\overline{R1}$ and $\overline{V1}$, and the original time of flight to compute a new $\overline{R2}$ and $\overline{V2}$ for the interceptor. There is also an iteration scheme in Subroutine KEPLER. This iteration is done to find the proper value of the x universal variable on the t vs. x curve. In this case, a Newton iteration scheme was chosen since there is not a well-defined interval on the t vs. x curve, as was the case with z in INTCPT. This technique involves guessing a value of x, using the slope of the t vs. x curve at that point and the deviation from desired time of flight (t) to determine the next trial value of x. It is a more efficient, but also more complicated, technique than bisection. It uses the fact that the slope of a tangent at the point in question is

$$\frac{dt}{dx} = \frac{\Delta t}{\Delta x} \tag{27}$$

which implies

$$\Delta x = \frac{\Delta t}{\frac{dt}{dx}} \tag{28}$$

and therefore

$$x_{n+1} = x_n + \frac{\Delta t}{\frac{dt}{dx}} \tag{29}$$

where

x_{n+1} is the new guess for x

x_n is the present guess

Δt is the deviation of t at x_n from the desired t

$\frac{dt}{dx}$ is the slope of the t vs. x curve at x_n

(14:87; 1:198)

The miss distance is the magnitude of the vector difference between the new target position and the new interceptor position. The error generations are repeated 500 times to compute a mean miss distance and delta V vs. acquisition distance for that trajectory. A feasible range of acquisition distances was established in Chapter II. Computation of delta V is accomplished as stated in the same Chapter.

In order to determine the statistical consistency of the results a standard deviation and variance for the mean miss distance is computed. The statistics gathered on the 500 iterations of the program itself use commonly accepted formulas as found in Probability and Statistics for Engineering and the Sciences by Jay L. Devore (3:22). In particular, for variance of a sample

$$\frac{\Sigma x^2 - (\Sigma x)^2/n}{n - 1} \tag{30}$$

the square root of which is the standard deviation of the sample.

The output of each run of the program is a mean miss distance over the 500 individual intercepts with standard deviation and variance, and delta V vs. acquisition distance for distances of 250, 500, 1000, 1500, and 2000 KM.

This discussion of the Program will now be augmented by a discussion of applications of the program and validation based on the author's experiences with the program in Chapter IV.

IV. Model Applications

Introduction

This chapter will explain the analyses which were performed to suggest possible uses for this model. All were done in a hypothetical sense, although every attempt was made to be as realistic as possible while maintaining the unclassified nature of the effort. The description will include how the input trajectory data was derived, how the error data was modeled, and specified sensitivity analyses that were performed.

Recall that this model is intended to be used as a "first look" evaluation tool for error assignment in a deep space ASAT system. Guidance errors and target tracking errors are evaluated over specified trajectories to determine the implications for ASAT sensor/maneuver subsystems. One might desire to estimate the delta V required based on the stated system and sensor capabilities and error values. This could then be transformed into a fuel weight to be added to payload weight to insure a launch vehicle is chosen which can lift that payload to the proper orbit. It is also possible to make inferences relating to the relative marginal returns of decreasing miss distance/delta V due to improvements in guidance and/or tracking of the target towards effective mission accomplishment. These are some of the ways this model could be put to use as one input in the tradeoffs of the decision process.

The Inputs

Scenario Vector Geometries. Four hypothetical targets were considered. No attempt was made to verify if any actual satellites are presently, or projected to be, in similar positions. Three of the four were in geosynchronous equatorial orbit. Target A was stationed over 100 degrees West Longitude, which cuts the continental United States approximately in half. This target was the initial baseline for experimenting with the model. Target B was stationed over 30 degrees East Longitude, which is very close to the Middle East and Eastern Europe. Target D was over 120 degrees East Longitude, which passes near to East and Southeast Asia. The fourth target (c) was a vehicle in a Molniya orbit, inclined 63.4 degrees to the equator, oriented so that apogee occurs alternatively over 30 degrees East and 150 degrees West.

Burnout for launches against the geosynchronous targets took place at 100 NM above the earth at 34.5 degrees North Latitude, 120 degrees West Longitude, when the 120 degree meridian was aligned with the vernal equinox direction so there is no J-component. Therefore, the burnout position vector ($\overline{R1}$) becomes

$$\overline{R1} = \frac{3543.934}{3443.934} \cos 34.5^{0} \; \overline{I} + \sin 34.5^{0} \; \overline{K} \qquad (31)$$

which becomes

$$\overline{R1} = .84803\overline{I} + .58283\overline{K} \qquad (31)$$

The 3443.934 is the mean equatorial radius of the earth (1:429). It is used to nondimensionalize the distance quantities to canonical units. Dealing in canonical units simplifies some of the constants used most commonly in many of the orbital equations (recall that the gravitational parameter "μ"=1 from Chapter II). It also lessens the chance of mixing metric and English units in the same equation. Development of the burnout vector for the Molniya case will be discussed later.

The direction of the $\overline{R2}$ vector, or projected target position, then is a function of the difference in longitude between $\overline{R1}$ and the longitude over which the target is stationed, and the amount of rotation of the object during the time of flight. For geosynchronous targets, this rotation amount coincides with the earth rotation rate (approximately 15 degrees per hour for these purposes). In the case of target A, there is a 20 degree difference in longitude and, for a 4-hour time of flight, an additional 60 degrees through which the vehicle must travel. Therefore, $\overline{R2}$ is a vector in the equatorial plane rotated 80 degrees counter-clockwise from the I-unit vector. The length of this vector can be determined from the formula for the period of an ellipse

$$tp = \frac{2\pi}{\sqrt{\mu}} a^{3/2} \qquad (32)$$

where

tp is the period of the orbit

"μ" is the gravitational parameter (its value is 1 in canonical units)

a is the length of the semi-major axis (the radius of a circular orbit)

Solving for a and assuming a period of 24 hours (107.08796 time units in canonical units), the radius of the geosynchronous targets is found to be 6.6228 DU (earth distance units). Knowing the direction and length of $\overline{R2}$, it may be represented in vector notation by

$$\overline{R2} = 6.6228 \cos 80^0 I + 6.6228 \sin 80^0 \overline{J} \qquad (33)$$

$$= 1.15\overline{I} + 6.5222\overline{J} \qquad (33)$$

The other geosynchronous target inputs can be computed in a similar fashion.

The Molniya case was handled slightly differently in that the intercept was assumed to take place at apogee, which for simplicity was assumed to be in the I-K plane. The $\overline{R1}$ vector was then "backed in" by figuring out where the burnout vector would be based again on time of flight and longitudinal difference between the two positions. Some resulting geosynchronous and Molniya inputs are shown in Table II.

Table II

Sample Trajectory Inputs (Target A & C)

Orbit Type	Time of Flight (TU)	R1 Vector (DU)			R2 Vector (DU)		
		I-Comp	J-Comp	K-Comp	I-Comp	J-Comp	K-Comp
Geo	13.386	.84803	0	.58283	2.7989	6.0023	0
Geo	17.858	.84803	0	.58283	1.15	6.5222	0
Mol	13.386	-.76857	.35839	.58283	3.2507	0	6.4916
Mol	17.858	-.64963	.54510	.58283	3.2507	0	6.4916

Error Models. Error characteristics for both the ASAT guidance and target tracking must be input in the Radial-Tangential-Normal reference frame. This reference frame was used because it is the way inertial guidance system characteristics are normally represented and also fit the characterization of target errors as well.

Mr. Dave Whitcomb at Aerospace Corporation was kind enough to provide data on some of our most widely used inertial guidance systems (IGS). This is shown in Table III. Notice there does not appear to be any strong correlation between any of the error terms (16). It was this observation which inspired the idea to model these guidance errors as spherically symmetric. This facilitated sensitivity analysis and permitted a more easily pictured perception of the kind of accuracies discussed. This is not an attempt to say that this representation would be appropriate in all cases, but it appears to be a good emulator in those cases considered here. Figure 4-1 shows sample results in the case of Target A for various times of flight.

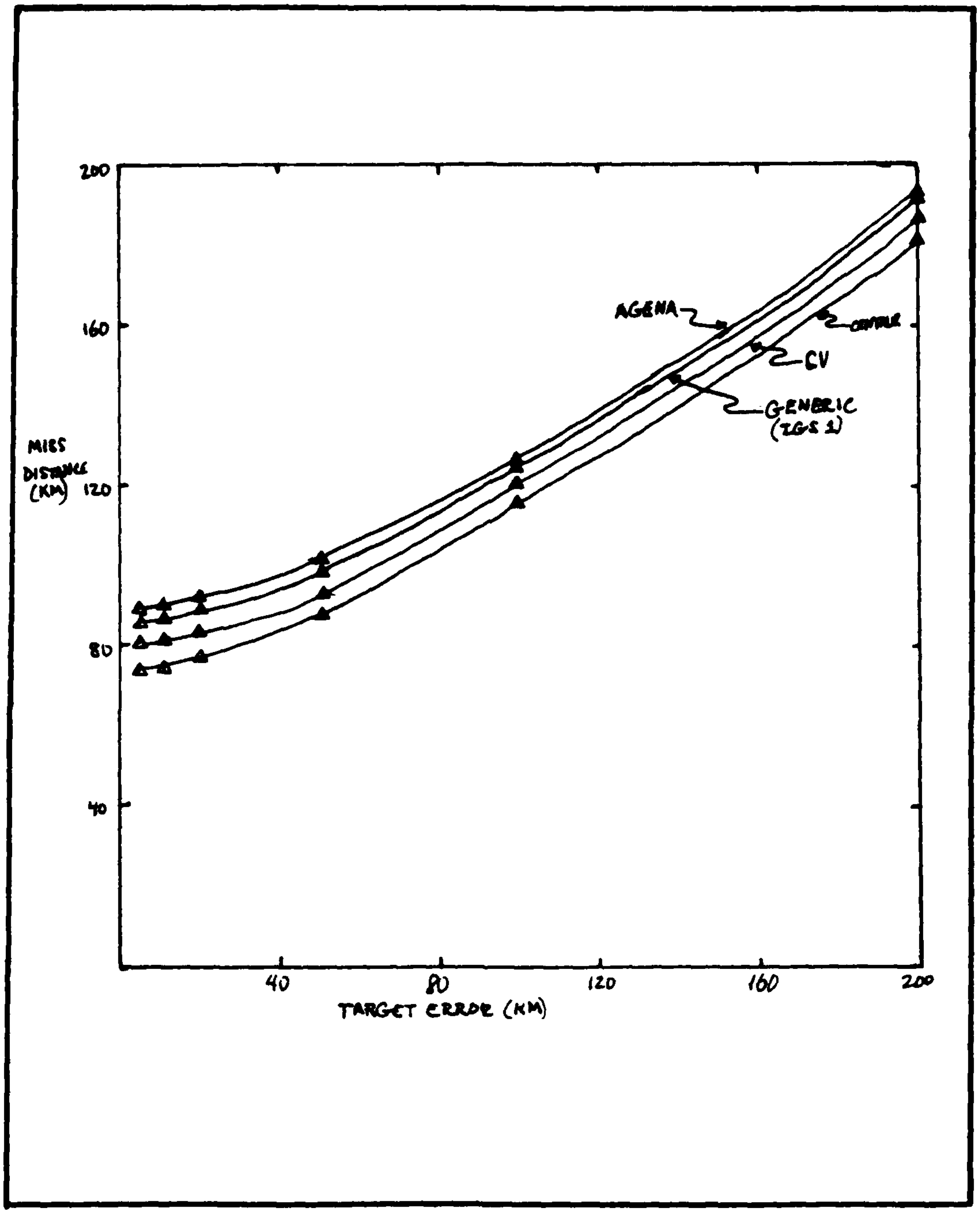

Figure 4-1. Comparison of Generic IGS Results to Actual System Data Results (Target A--4 Hour TOF)

Table III

Injection Errors (1 sigma) for 3 IGS's
with Burnout Velocity 35,000 fps.

	Carousel V	Centaur Platform	Agena AGS	Units
R	2664	4460	2493	ft
T	7206	5412	4430	ft
N	6841	6313	4426	ft
$\dot{R}$	8.024	4.960	9.49	fps
$\dot{T}$	4.270	5.204	3.31	fps
$\dot{N}$	3.117	8.130	7.21	fps

(16)

The target tracking errors were also modeled in the R-T-N system after consultations with deep space experts from Lincoln Laboratory and the Cheyenne Mountain Complex. While numerical estimates of accuracy vary from target to target due to such things as location and sensor coverage, these experts agreed that most of the position error is "in track," along the trajectory. This coincides with the tangential component of R-T-N. For this reason, and for lack of any better approach, target errors are modeled based on a normal distribution in the tangential component, with the normal and radial components "scaled" an order of magnitude less than the tangential. For example, when a target error of 20 KM, 1 sigma, is specified, the scaling factors would be 20 KM in the tangential direction and 2 KM in each of the radial and normal directions. This will result in an error ellipsoid with its major axis oriented along the tangential axis, centered at the vehicle's projected position. This is an area which could be explored further if time allowed. The "order of magnitude" scaling is an approximation based on the author's interpretation of the experts descriptions. More importantly, when a real world specific target is identified, its particular error characteristics can be more easily described due to knowledge of its location, sensor access, latest "tracks," and historical data about whether it is prone to maneuver (5).

The only remaining input is the projected target velocity vector at intercept. It is necessary to transform the R-T-N error components to the I-J-K system so that those components can be added directly to the appropriate vector. With knowledge of the target's orbital parameters, the velocity vector can be expressed in the perifocal coordinate system with the following equation:

$$\bar{V} = (\mu/p)^{\frac{1}{2}} \left[-\sin \nu \, \bar{P} + (e + \cos \nu) \, \bar{Q}\right] \tag{34}$$

A complete understanding of the perifocal system is unnecessary for this development, but the curious reader can find it in Bate's Chapter 2 (1:57). The important feature is that the above vector can be transformed to the I-J-K system with use of a 3x3 transformation matrix R whose elements are:

$$R_{11} = \cos \Omega \cos \omega - \sin \Omega \sin \omega \cos i \tag{35}$$

$$R_{12} = -\cos \Omega \sin \omega - \sin \Omega \cos \omega \cos i \tag{36}$$

$$R_{13} = \sin \Omega \sin i \tag{37}$$

$$R_{21} = \sin \Omega \cos \omega + \cos \Omega \sin \omega \cos i \tag{38}$$

$$R_{22} = -\sin \Omega \sin \omega + \cos \Omega \cos \omega \cos i \tag{39}$$

$$R_{23} = -\cos \Omega \sin i \tag{40}$$

$$R_{31} = \sin \omega \sin i \tag{41}$$

$$R_{32} = \cos \omega \sin i \tag{42}$$

$$R_{33} = \cos i \tag{43}$$

where

i is the orbital inclination

ω is the argument of perigee

Ω is the longitude of the ascending node (the angle between the I-vector and the point where the satellite passes through the equatorial plane in a northerly direction) (1:82).

In the case of the geosynchronous equatorial orbit, this transformation matrix becomes the identity matrix. In the case of Molniya, both the argument of perigee and the longitude of the ascending node are 270 degrees, so it also simplifies considerably. One might ask how much error might be induced by the fact that the true position of the satellite is not where it is assumed to be for these computations. In both orbit classes the velocity vector is perpendicular to the position vector at the point in question. The target tracking errors under consideration are all less than 200 KM, which translates to about 0.25 degree or less difference between the two position vectors. This is also the deviation between the two velocity vectors since each is perpendicular to its respective position vector. The effect is, therefore, insignificant.

In conclusion, the inputs to the program are:

1. ASAT initial position vector (I-J-K components)
2. Projected target position at intercept (I-J-K components)
3. Time of flight for intercept
4. Projected target velocity vector at intercept (I-J-K components)
5. Expected position error characteristics of launch vehicle guidance at burnout (1-σ values for R-T-N components)
6. Expected velocity error characteristics of launch vehicle guidance at burnout (1-σ values for R-T-N components)
7. Target tracking error characteristics (1-σ values for R-T-N components)

(All entries in earth-based canonical units)

The Applications

Before launching into some hypothetical scenarios for applications, it might be helpful to review the general philosophy of the approach to this problem. The suggestion that there was a need to have a model such as this came from individuals concerned about the relative inadequacy of the U.S. deep space surveillance capability vis a vis near space. It was felt that a tool which could help examine the implications of these inadequacies would be helpful in any consideration of new deep space ASAT systems. In order to keep this document unclassified, the author attempted to keep all capabilities in a "generic" vein rather than model specific system entities. Therefore, all the guidance errors considered involve the "spherical symmetry" developed earlier; target errors incorporate the "elongated ellipsoid--order of magnitude" approach; and various ASAT subsystem possibilities were considered.

In a general application, Program ASAT can be used to gain overall insight into the interactions of the errors that are modeled. For example, if one wishes to get an understanding of the marginal returns of improved IGS accuracy vs. improved target tracking accuracy, miss distance is a good metric to use. This would take the form of a sensitivity analysis. That is, make a series of runs where all inputs are held constant except one, and the results will show the sensitivity of miss distance to that parameter. In this case, sensitivity analysis for both IGS accuracy and target tracking were done to determine under what circumstances one of them provides a better performance payoff than the other. Now consider some examples of these "trend identifying" applications as applied to the targets A-D.

The four targets were baselined with the "generic" IGS which produced results similar to the data obtained from the Aerospace Corporation when various target error values and 3 and 4 hour times of flight were used. As mentioned, the six components of IGS error were all decreased incrementally (as a unit) to determine the effect of an improved IGS. One representative sample result is shown in Figure 4-2. For this example the miss distance shows that an order of magnitude improvement in IGS error eliminated the IGS as a source of error when target errors were in excess of 5 KM (1-sigma tangential). Four generic classes of IGS errors were then selected: the baseline (2.4×10^{-4} for each of the six components), an order of magnitude better (2.4×10^{-5}), and two values between those two (1.32×10^{-4} and 5×10^{-5}). The results of running the four IGS classes and various target error classes (1, 5, 10, 20, 50, and 100 KM 1-sigma tangential) for each of the four targets and a three hour time of flight, are shown in Figures 4-3 through 4-6. In these figures miss distance is plotted as a function of IGS accuracy in the left graph, and as a function of target tracking accuracy in the right graph. Note the basic similarity of the plots between targets, including the Molniya. The following inferences can be made from these results:

1. If the IGS is limited by other factors to no better than 10^{-4} (1-σ across all components of position and velocity), there is no payoff for improving tracking from 10 KM to 1 KM, and very little payoff from 20 KM to 1 KM. That conclusion can be drawn due to the closeness of the 1, 5, 10, and 20 KM lines in Figure 4-3 (left) and the leveling off of the top two curves of Figure 4-3 (right).

2. If the target list includes targets with tracking errors in excess of 50 KM (1-σ tangential), relatively limited payoffs are possible with improved IGS. This can be seen in the closeness of the IGS lines in Figure 4-3 (right)

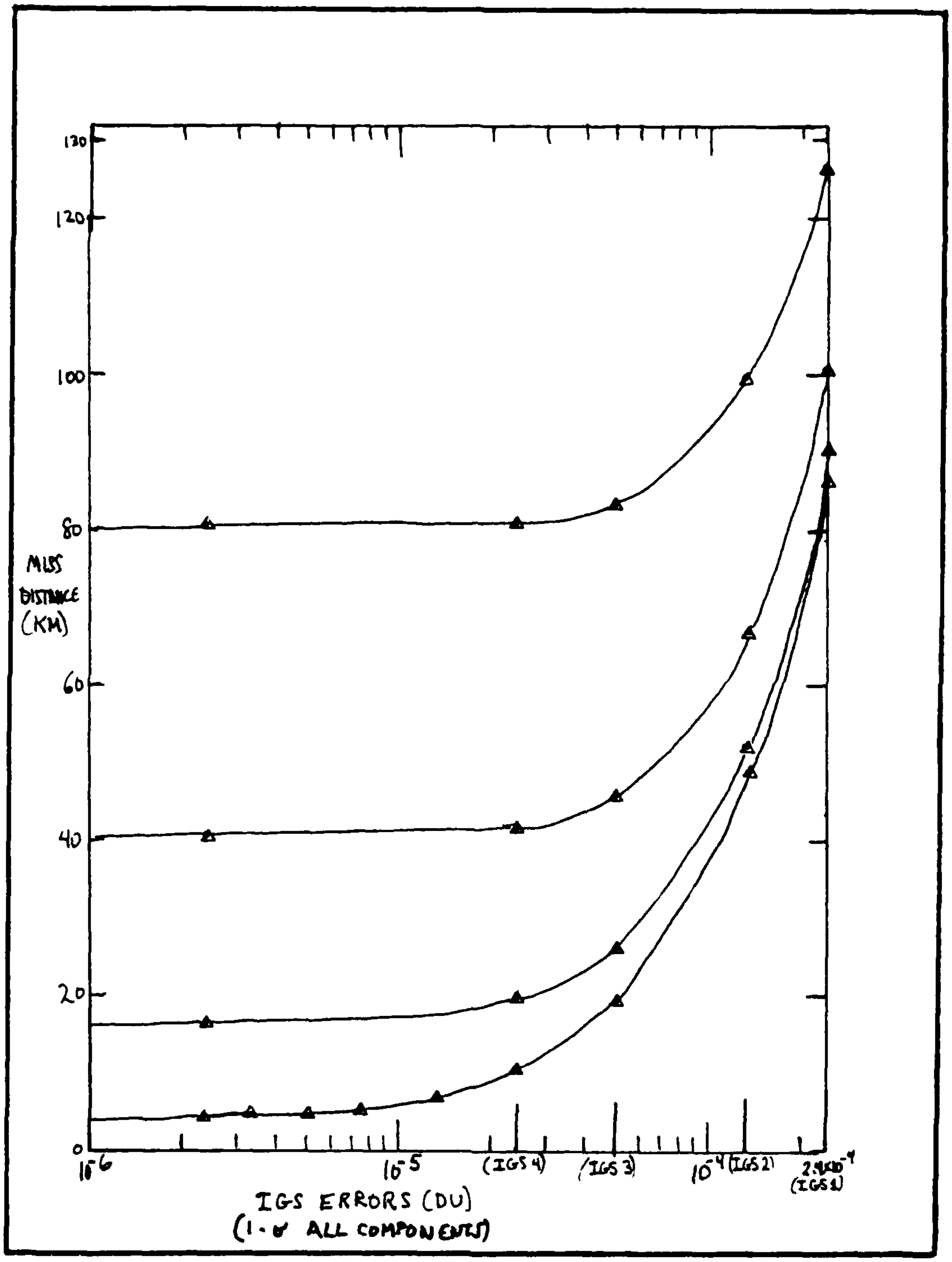

Figure 4-2. Miss Distance vs. IGS Accuracy
(Target A--4 Hour TOF)

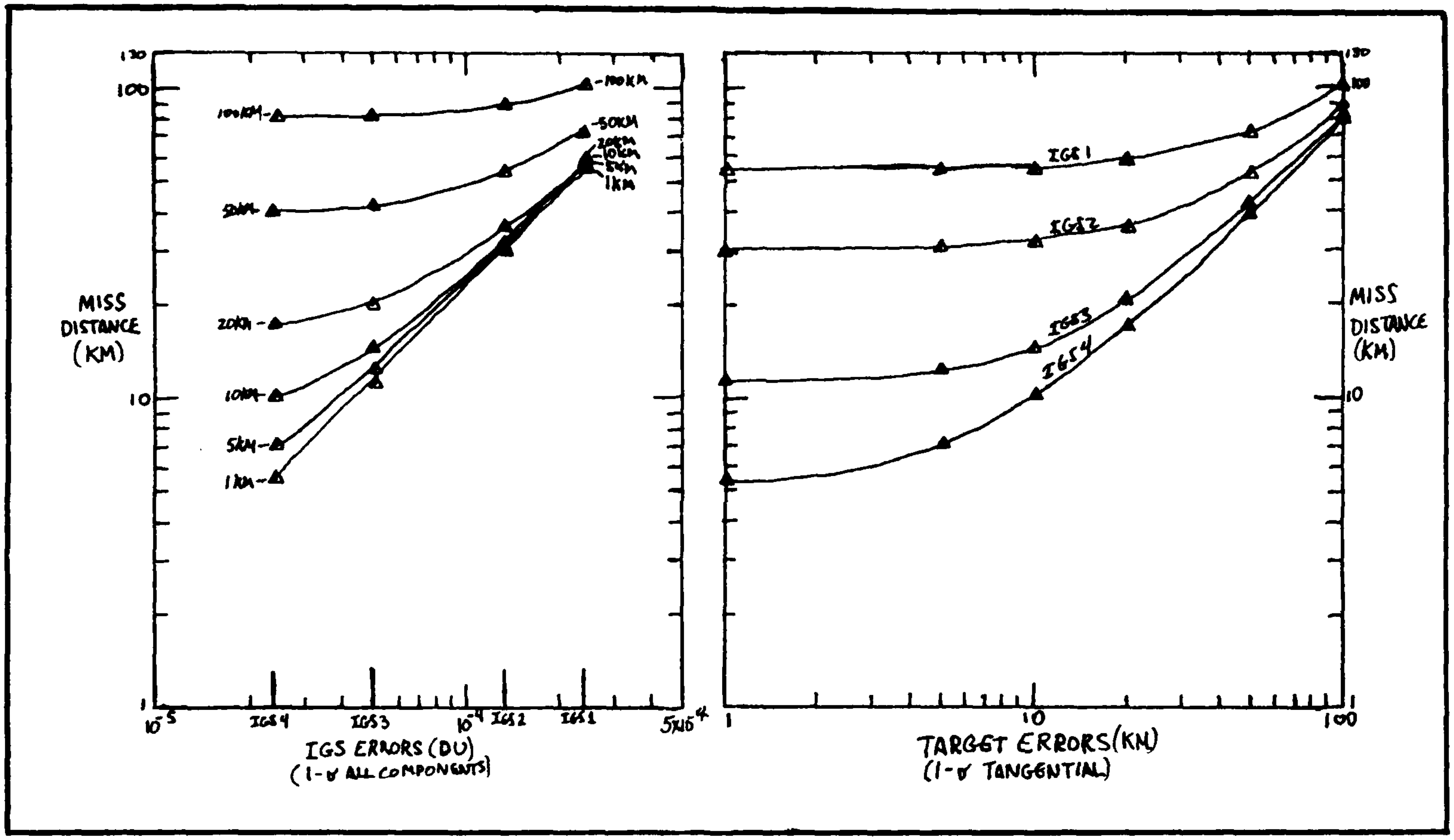

Figure 4-3. Miss Distance as a Function of IGS Accuracy (Left) and Target Errors (Right) (Target A--3 Hour TOF)

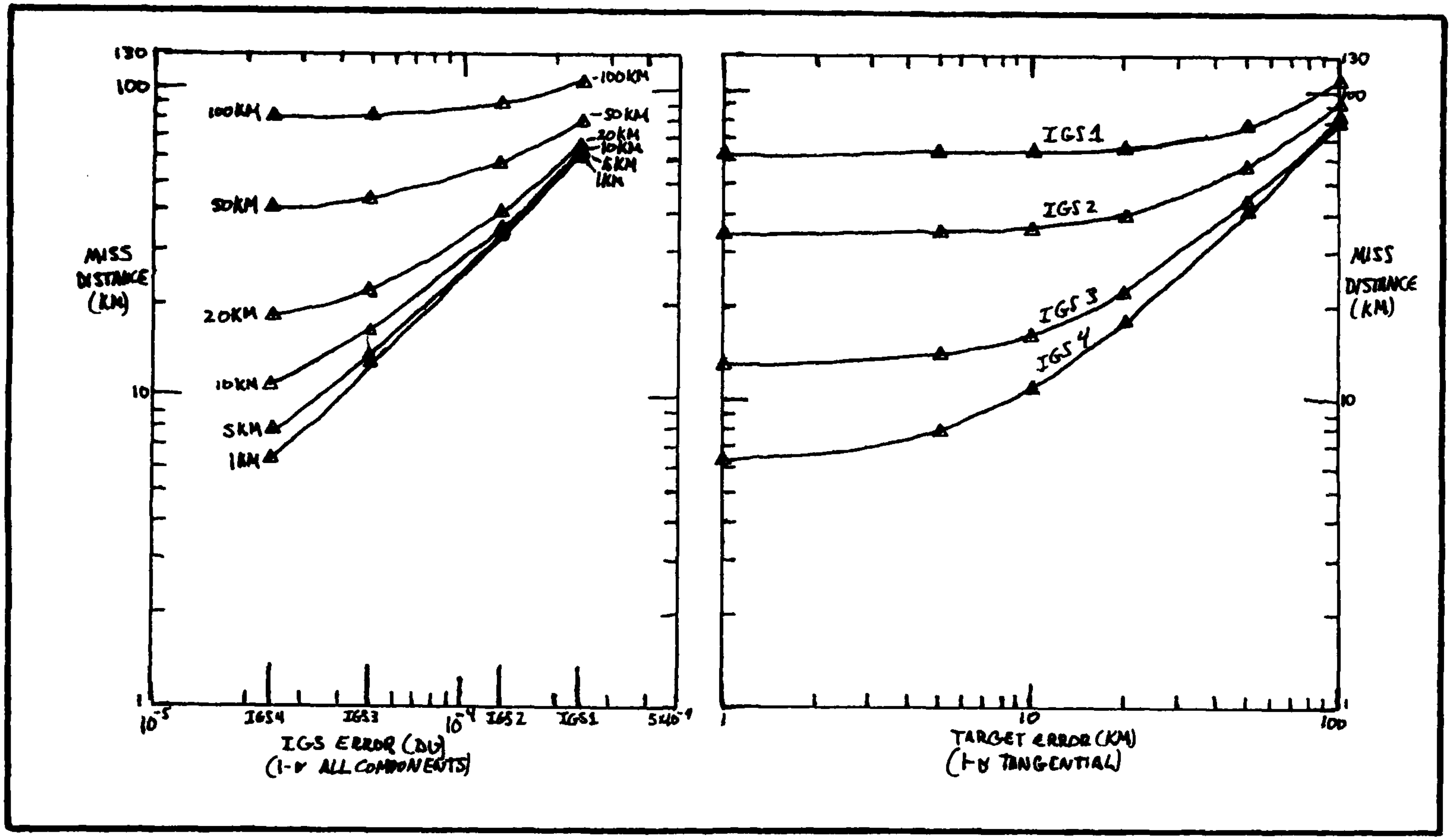

Figure 4-4. Miss Distance as a Function of IGS Accuracy (Left) and Target Errors (Right)
(Target B--3 Hour TOF)

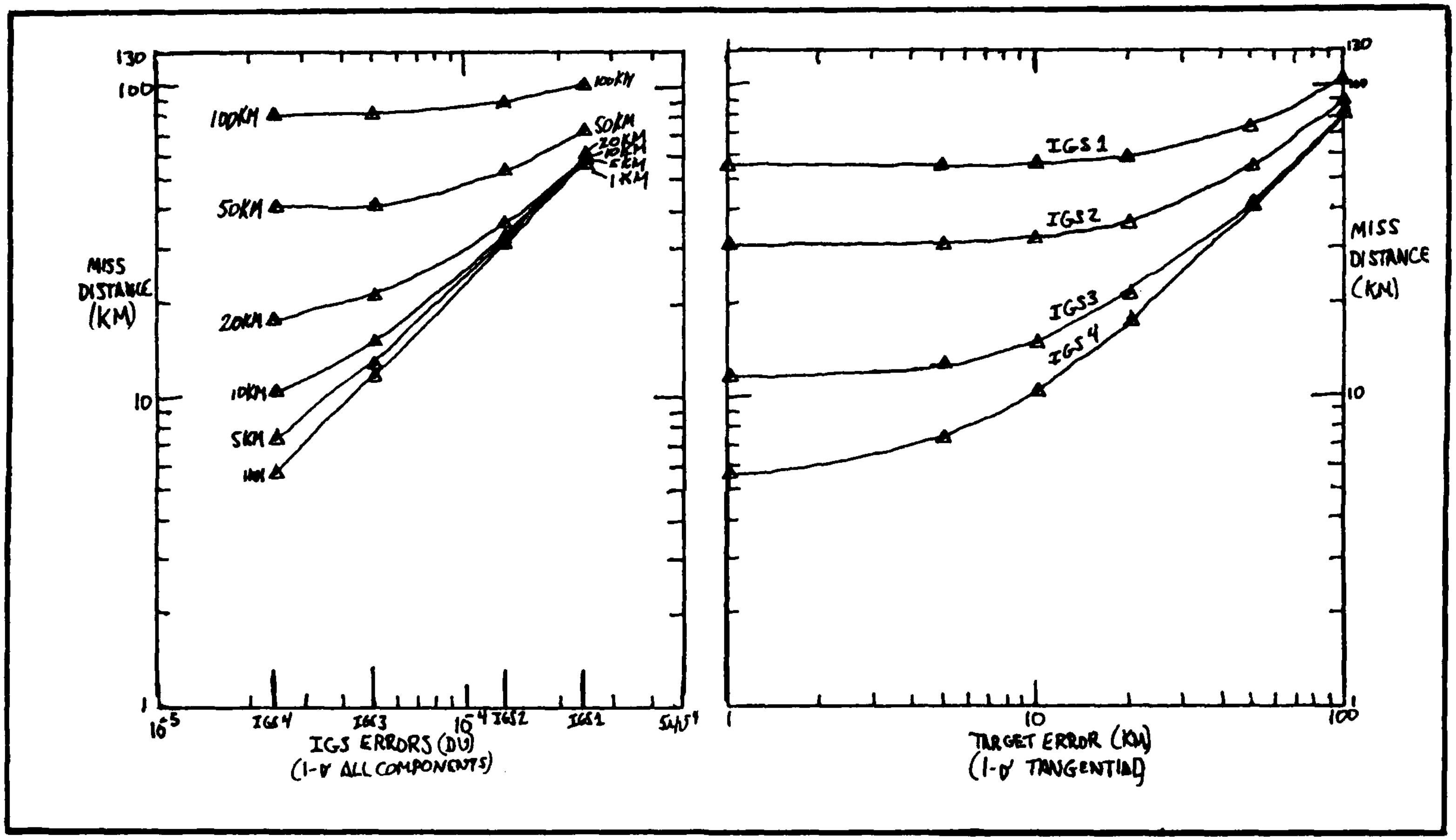

Figure 4-5. Miss Distance as a Function of IGS Accuracy (Left) and Target Errors (Right)
(Target C--3 Hour TOF)

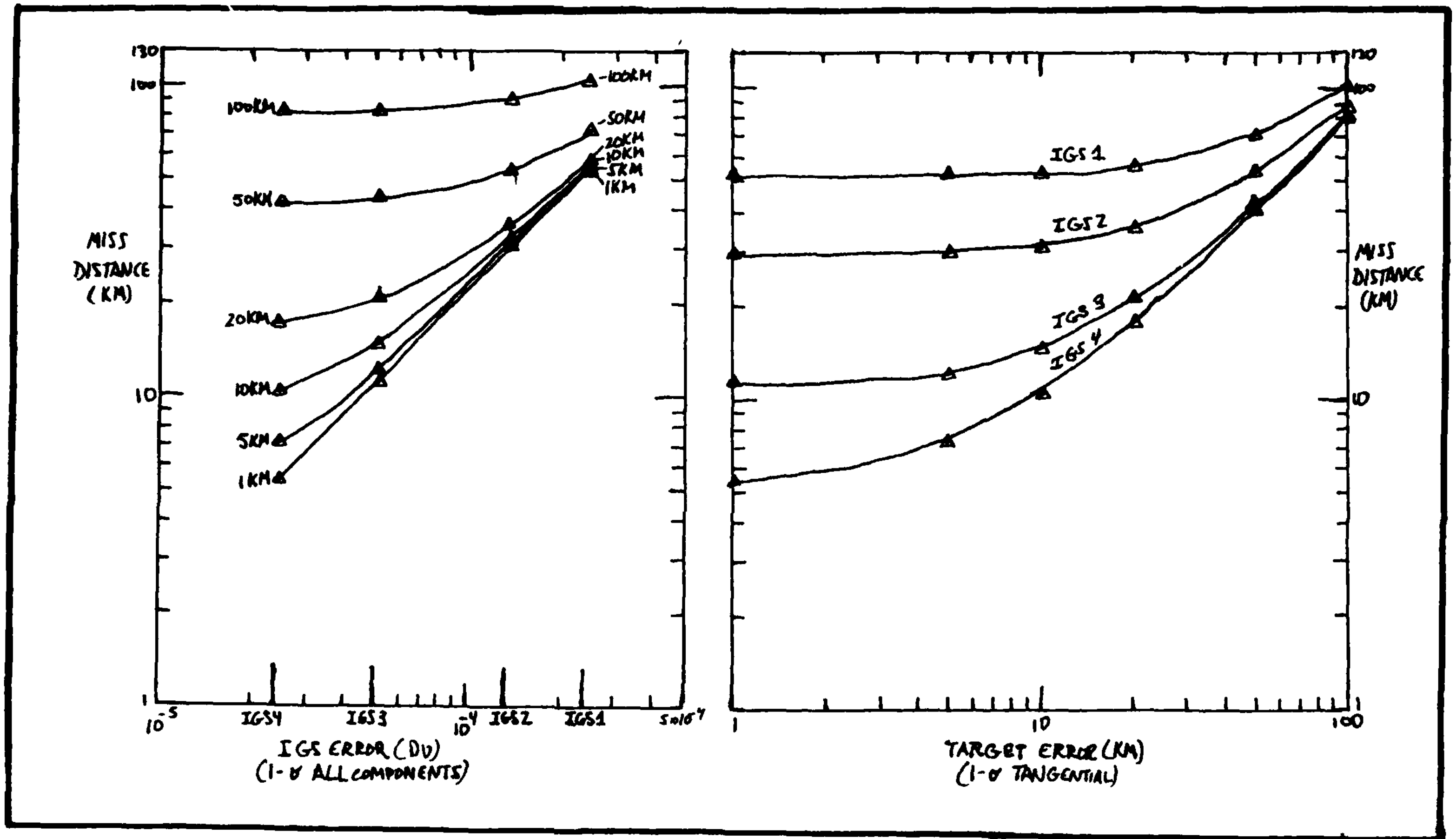

Figure 4-6. Miss Distance as a Function of IGS Accuracy (Left) and Target Errors (Right)
(Target D--3 Hour TOF)

> and the quick leveling of the 50 and 100 KM lines in Figure 4-3 (left). This can also be seen in Figure 4-7 which shows delta V vs. acquisition distance for various target errors and IGS 1 and 4. This shows how delta V may also be used to gain these insights.

Now consider changing the time of flight to Target A from three to four hours. These results are shown in Figure 4-8. Miss distance shows a greater sensitivity to a one hour time of flight change than to large differences in orbital position of target. Therefore, the timelines stated in the operational concept could be significant drivers in the error assignment process. This is particularly true in the cases when IGS errors are significant because the resultant errors are more sensitive to time of flight. This is as expected, since target errors are not affected by time of flight and, the longer it takes the ASAT to get to the target, the farther the induced IGS errors will vary from the nominal. This illustrates the "trend indicator" uses for Program ASAT, which can be very valuable, especially early in the system life cycle.

Program ASAT can also be used for more system specific purposes. For these purposes the delta V output is a useful measure. The delta V may be used in the rocket equation to solve for the mass of fuel required to impart the required velocity increment. This is important when considering the total payload weight that must be launched. With that in mind, the three scenarios that follow are examples of how the Program may be used in more system/subsystem oriented tradeoffs.

Scenario One. Suppose the user defines the target list as shown in Table IV. The IGS chosen is to be either number 1 or number 2 from the classes discussed earlier. The user has determined that for this level, the 1000 KM sensor acquisition is the criteria for judging delta V

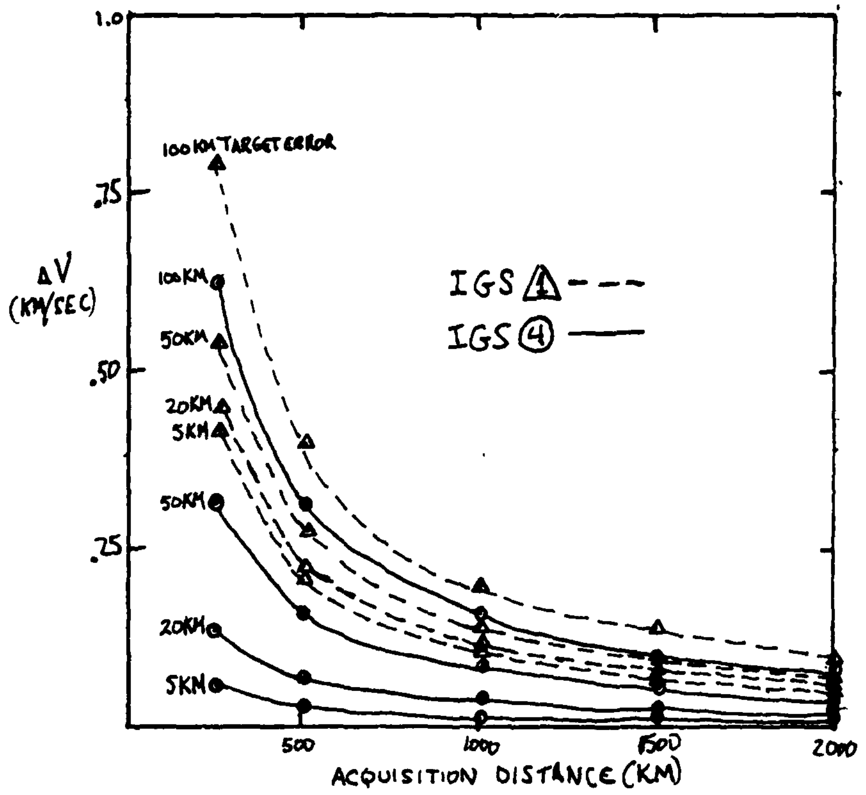

Figure 4-7. Delta V vs. Acquisition Distance
(IGS 1 and IGS 4, Various Target Errors, 3 Hour TOF)

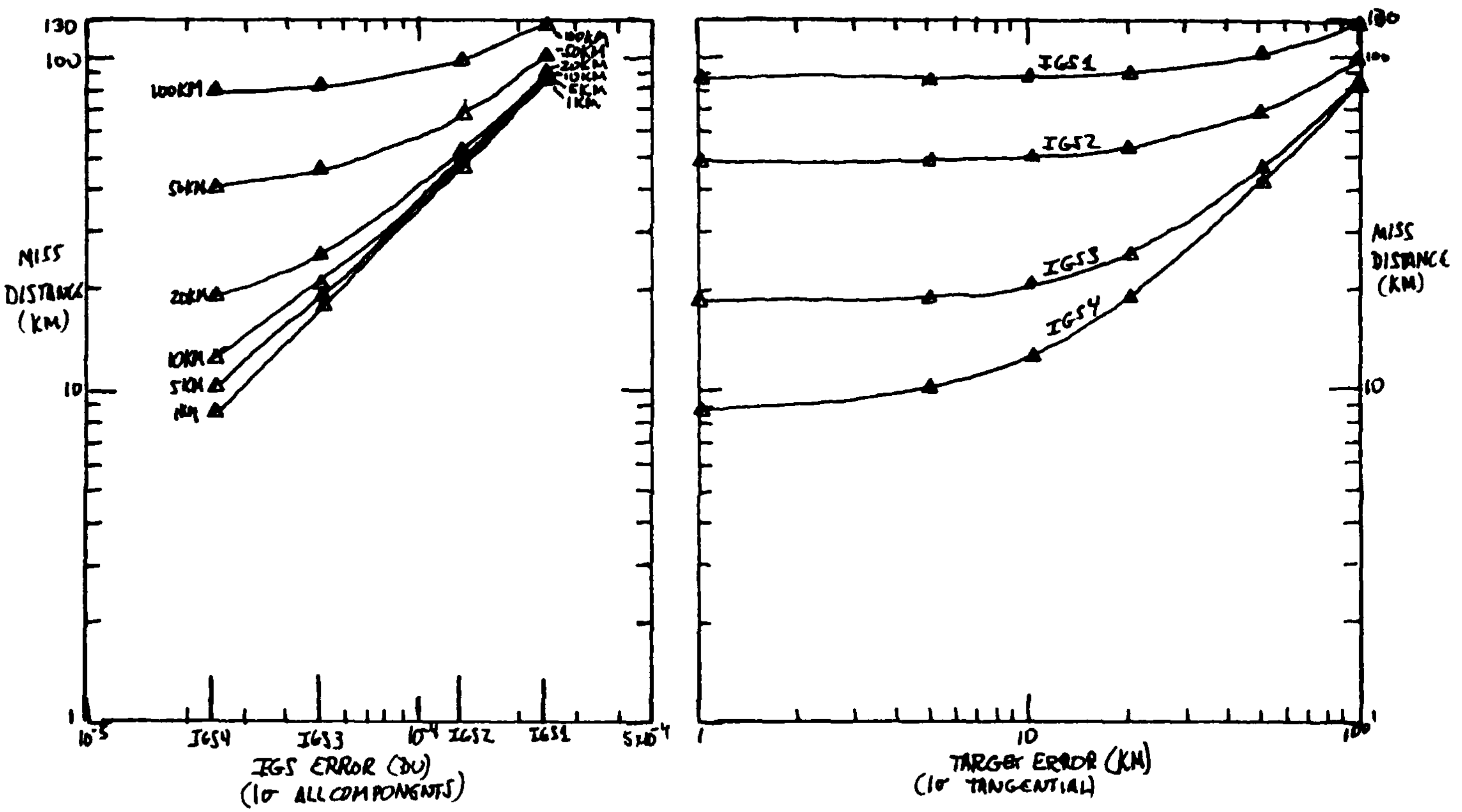

Figure 4-8. Miss Distance as a Function of IGS Accuracy (Left) and Target Errors (Right)
(Target A--4 Hour TOF)

requirements. The ASAT vehicle under consideration has an initial mass of 500 kg, with a nozzle exit velocity of 3 KM/sec. Based on this input data, Target B has the highest delta V requirement of 0.17676 KM/sec for IGS 1, while Target C is the highest for IGS 2 at 0.10951 KM/sec. Using the rocket equation:

$$\frac{\Delta V}{V_e} = \ln \frac{mi}{m_f} \tag{44}$$

where

ΔV is the velocity increment change

V_e is the exit velocity of exhaust gases from nozzle

m_i is initial mass of vehicle

m_f is final mass of vehicle

we find that about 30 kg of fuel will be sufficient with IGS 1 while about 19 kg are required with IGS 2. In this case, the difference is not very great and, depending on the lift capability of the launch vehicle, may be inconsequential, so the older, proven (and probably cheaper) IGS 1 would be preferred for this one input to the bigger decision process.

Table IV

Scenario One

Target	Error (KM) 1-σ tang	ΔV (KM/Sec) for 1000 KM Acq. Dist.	
		IGS 1	IGS 2
A	10	.10604	.06053
B	20	*.17676	.10692
C	50	.14777	*.10951
D	20	.14188	.08789

Scenario Two. Now suppose for the same situation as Scenario 1 except the conservative approach is taken for the sensor, and the 250 KM figure is the judging criteria (See Table V). The same two targets are the drivers, but now Target B requires 0.70704 KM/sec for IGS 1 and Target C requires 0.43805 KM/sec for IGS 2. This results in a requirement for 133 kg of fuel with IGS 1 and 79 kg with IGS 2. In this case, a difference of over 50 kg might well impact the mission and influence these tradeoffs.

Table V

Scenario Two

Target	Error (KM) 1-σ tang	ΔV (KM/Sec) for 250 KM Acq. Dist.	
		IGS 1	IGS 2
A	10	.42417	.24213
B	20	*.70704	.42769
C	50	.59108	*.43805
D	20	.56752	.35157

Scenario Three. In this case, we have the same basic ASAT characteristics as Scenario Two, but now the guidance system is IGS 4 (See Table VI). In this case, we have options available to improve tracking accuracy on all targets to 1 KM (1-sigma tangential). The driving delta V's are 0.33252 (Target C), with the tracking specified previously, and 0.06793 (Target B) with the improved tracking. The fuel required is now 59 and 11 kg, respectively, another 50 kg difference.

Table VI

Scenario Three (IGS 4)

Target	ΔV (KM/Sec) for 250 KM Acq. Dist.	
	Previous Errors	1 KM (1-σ tang)
A	.07837	.04243
B	.19443	* .06793
C	*.33252	.04548
D	.17565	.05385

These Scenarios and the previous general trend examples are hypothetical in nature, but they are illustrative of the way this model can be used as one measure of evaluation of different options. Of course, this is only one element of system tradeoffs which must be considered in the context of the whole system, but it provides a measure for performance tradeoffs to be considered in consonance with such factors as cost, schedule, and technical risk.

Validation

Model validation begins with the realization that the model is not intended to duplicate exactly any real world event. Additionally, since there is to date no actual deep space Anti-satellite system, there are no real world performance results. Finally, the author is unaware of any other model which might be used in lieu of a real world system. For these reasons validation is achieved with the "towards-validation" approach suggested by Ghelber and Haley (4). Ghelber and Haley define "towards-validation" as, "the documented evidence that a computerized model can provide users verifiable insight, within the model's domain of application, for the purpose of formulating analytical or decision-making inferences" (4:13).

The process involves a four phased approach:

1. Conceptual
2. Verification
3. Credibility
4. Confidence

Conceptual. The four basic elements of this phase are as follows (4:15):

1. A formal written statement of the intended application of the model.
2. Specification of the degree of accuracy required.
3. Description of assumptions and limitations.
4. Structural model or framework for design development.

The first three of these elements are described in the "Scope and Assumptions" section in Chapter I. The structural model was included in Chapter III.

Verification. This phase is concerned with the "mechanical validity" of the model and four steps are suggested (4:19):

1. Structured walk-through.
2. Verification of technical physical processes.
3. Simulation of predictable results.
4. Testing of stochastic events.

The intent of the structured walk-through is to verify correct data manipulation and build confidence in the mechanical structure by hand calculating and manually tracking data through the model. This process was followed in the development of each of the subroutines by printing intermediate results of each computational step in the early runs. In addition, the orbital prediction subroutines were verified by use of sample problems and answers given in Bate (1:210,236). Each subroutine was also used "against" the other. In other words, a given $\overline{R1}$, $\overline{R2}$, and time input to INTCPT, will result in output of $\overline{V1}$ and $\overline{V2}$. Using that $\overline{R1}$, $\overline{V1}$, and time as inputs to KEPLER, should result in output of the same $\overline{R2}$ and $\overline{V2}$. Conversely, input of $\overline{R1}$, $\overline{V1}$, and time to KEPLER, results in output of $\overline{R2}$ and $\overline{V2}$. $\overline{R1}$, $\overline{R2}$, and time may then be used in INTCPT to get $\overline{V1}$ and $\overline{V2}$ which should check with $\overline{V1}$ and $\overline{V2}$ from the KEPLER run.

Verification of physical processes involves "insuring that the proper equations and relationships are used in developing the model" (4:20). It has already been stated that the astrodynamic routines were taken from a text book and the implementation into Program ASAT was verified as cited above. The random number generator used a technique from *Systems Simulation: The Art and Science* by Shannon in application of the central limit theorem to convert random numbers from a uniform distribution to a standard normal distribution (10:362). The particular method chosen "does very poorly in generating the tails of the normal distribution" (10:363). However, as previously mentioned, this was found to have negligible effects on the results.

Simulation of predictable states is an attempt to verify that certain "predictable" events produce the "predicted" results. This was accomplished through several tests. One test was to introduce near-zero errors to produce the expected zero miss distance and zero delta V. Near-zero was used because input of zero itself would result in dividing by zero. In this case, 10^{-20} was used which is about 15 orders of magnitude less than any input error parameters. Simulation results showed a miss distance of 2 cm. This is negligible considering the distance traveled is over 35000 KM (9 orders of magnitude difference), and the target is no smaller than one square meter. The 2 cm may be due to slight computational differences in the two orbital prediction subroutines. Another test was to increase the guidance error input parameters. Increasing the guidance error input parameters increases the miss distance and delta V outputs. Decreasing the same parameters produced decreasing miss distance and delta V. In fact, as the guidance errors propagate linearly, it was confirmed that, with no target errors involved, doubling the input guidance error parameters doubles the output miss distance.

Testing of stochastic events is the final step of the verification phase. The random generator as previously described is a commonly accepted technique and was verified even to the point of plotting the distribution. Even more importantly, varying the random number seed did not significantly change any outcomes. Therefore, the random generation technique itself does not affect the results substantially.

Credibility. This phase attempts to improve "both the intuitive and the statistical appeal of the model based on face validation and sensitivity analysis" (4:22).

The approach for face validation was to present the model to experts in the specific subject areas involved to get their opinion of shortcomings or problem areas. The following individuals were consulted in the areas shown:

> Dr. William Weisel - Model Structure, Astrodynamics, Error Generation
>
> Maj. Joe Coleman - Error Generation, Statistics
>
> Both have concluded that the model is sound technically.

Sensitivity analysis is a major item discussed in the "Applications" section earlier in this Chapter. That discussion established sensitivity of miss distance to varying time of flight. It also established a lesser sensitivity to varying longitude of geosynchronous type targets when time of flight is constant. This leads to the conclusion that timelines established by the operational concept could be real drivers in system error assignment. However, as with any model, but especially one created in an academic environment with absolute time constraints, there is always more that can be done. One of the analyses to be considered deals with the sensitivity to changes in guidance error parameters and tracking error parameters as applied to a few select intercept trajectories. More trajectories could be considered especially with regard to varying time of flight. More detailed analysis of guidance error parameters is another area where further efforts are in order. In particular, the position and velocity components, which were considered as one entity, could be analyzed separately.

Confidence. Ghelber and Haley contend that confidence building begins with the first steps in the conceptual phase and continues through all the previously mentioned model building and use (4:29). Two of the recommended steps in this phase are:

1. Statistical comparison of modified simulation runs with related data.
2. Full documentation of the towards-validation process.

In all the runs of various target scenarios, and guidance and target error combinations, the statistical consistency of the model has prevailed. The following equation is used to compute the interval about the sample mean (miss distance) within which the true mean is located to a confidence of 95%:

$$\bar{x} - \frac{1.96\sigma}{(n)^{\frac{1}{2}}} < \mu < \bar{x} + \frac{1.96\sigma}{(n)^{\frac{1}{2}}} \qquad (45)$$

where

$\bar{x}$ is the sample mean

μ is the true mean

σ is sample standard deviation

n is the sample size (3:320)

Application to the runs conducted in this analysis consistently showed the true mean to be within 0.1% of the sample mean. Table VII shows a sample of results.

Table VII

Sample Results for Test of Sample Means (95% Confidence)

Target	IGS#	Target Error (1σ tang)	% Deviation
A	1	1 KM	.07
A	3	20 KM	.06
B	2	50 KM	.05
C	4	100 KM	.07
D	1	100 KM	.06

Full documentation of all efforts to establish validation with the towards-validation approach has been the goal of this section.

Summary

While recognizing that the model does not completely emulate the real world, it achieves its design purpose quite well. That purpose is to serve as a first order error assignment model for decision makers as they begin to consider candidate deep space anti-satellite systems. However, more insight into error assignments might be achieved with applications work in the area of sensitivity analysis and other target orbits (e.g. half synchronous).

V. Conclusions and Recommendations

Conclusions

A model has been developed which is capable of serving as an evaluation tool in first order approximation error assignment for deep space ASAT targeting. It is a model which can be used as an aid in measuring system performance. With that aid, more informed decisions can be made with regard to total system tradeoffs in such areas as cost, schedule, performance, and technical risk. Figure 3-2 is repeated here to emphasize where Program ASAT fits into the systems development process.

An examination of the objectives stated in Chapter I reveals that this effort has succeeded in its purpose. In that regard it is a first step toward understanding deep space targeting problems. The utility of the model has been described in Chapter IV. It should also be noted that each run of the program takes approximately 1.5 seconds of compile and execution time on the Cyber computer. This means numerous runs can be performed in a reasonable amount of computer time, which permits more "what if's" to be considered. It is recognized and encouraged that further efforts be made to improve and expand the applications and capabilities beyond those stated here. To that end, there are several specific recommendations which may inspire further efforts.

Recommendations for Follow-On Work

One area for study involves the modeling of target errors. Is there a better way to model these errors than the "1-sigma tangential elongated ellipsoid" used here? This approach was used based on the experience and opinions of some experts in the field. However, no detailed analysis was

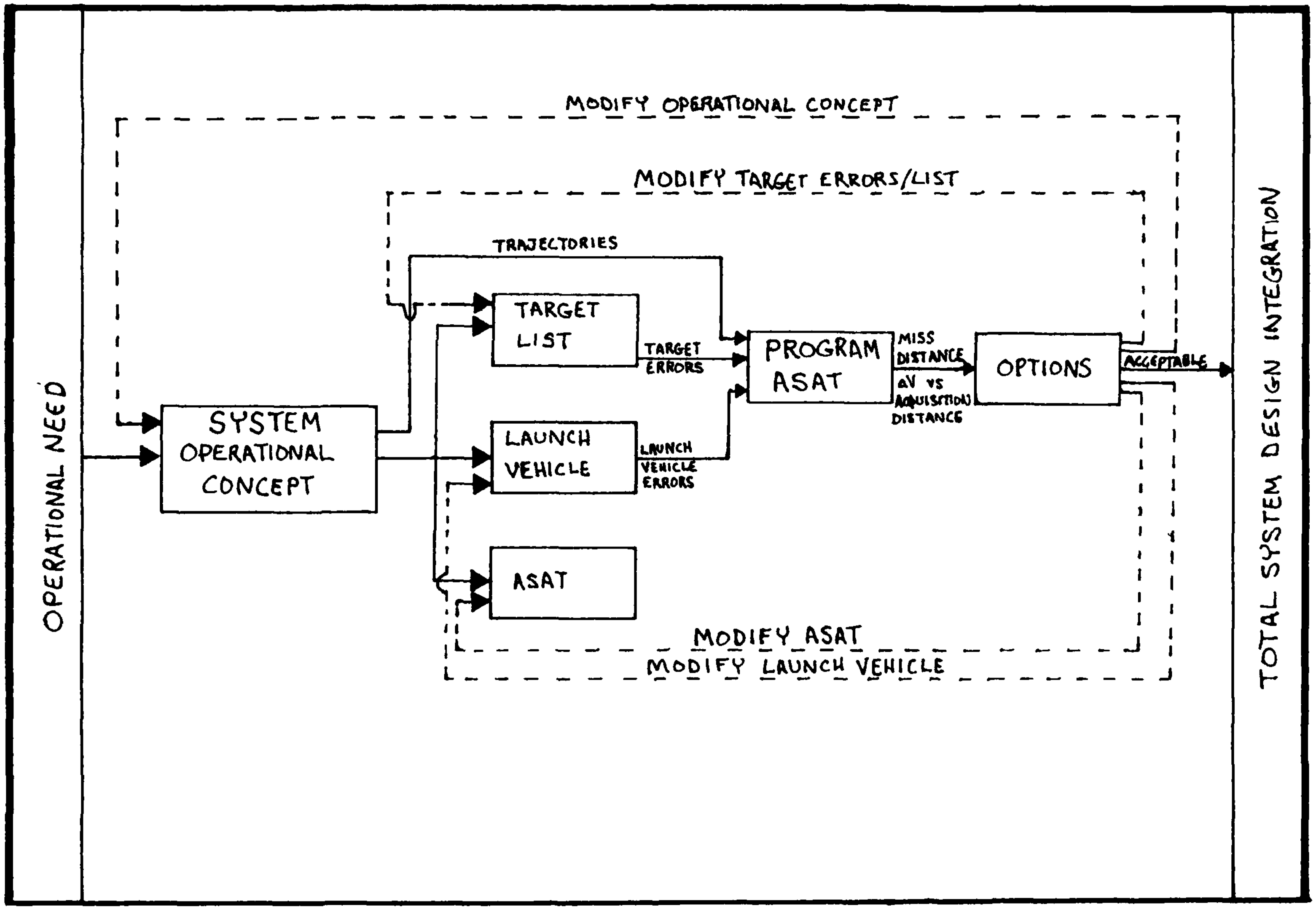

Figure 3-2. Program ASAT's Role in Performance Tradeoffs

performed, nor were these experts aware of one, which could confirm this approach or suggest a better way.

In Chapter IV the launch vehicle errors were mentioned as an area worthy of further study. Additional sensitivity analysis treating the position and velocity entities separately rather than as a unit could be done. Is there any greater payoff for improvements in position over velocity, or vice versa?

An important area for follow-on efforts to extend the utility of Program ASAT is that of a maneuvering target. Once adversaries know that deep space satellites are likely to become targets of an ASAT, they certainly will consider a maneuver capability as a counter measure. Even before something like that could be incorporated in Program ASAT, some study of the nature of likely maneuvers would need to be accomplished. Orbital mechanics limits those maneuvers to some degree. Beyond that, one must make a judgment as to how much of a maneuver is likely from a mission standpoint. This knowledge, coupled with knowledge of Spacetrack coverage, may enable us to better predict and be prepared for evasive action.

Further examination of the "mean miss distance" as a measure of performance is another area any user may consider for more detailed study. It is a good measure for the general "trend-indicator" uses described earlier, but, in more system specific cases, the user may want to consider how that mean translates to a success rate for intercept. In the cases considered here, it appears that designing to the mean will succeed in about 65% of the Monte Carlo generated intercepts. A user could examine the distribution of the subject miss distances to make a determination of what specific criteria would be sufficient for his/her purposes.

Bibliography

1. Bate, Roger R., Donald D. Mueller, and Jerry E. White. Fundamentals of Astrodynamics. New York: Dover Publications, Inc., 1971.

2. Becker, Maj Evan S., Directorate of Space Systems, Space Command. Memo for Record: SPADATS Deep Space Tracking Accuracies, 13 May 1983.

3. Devore, Jay L. Probability and Statistics for Engineering and the Sciences. Monterey, California: Brooks/Cole Publishing Company, 1982.

4. Ghelber, Craig S. and Charles A. Haley. "A Methodology for Validation of Complex Multi-Variable Military Models." Unpublished MS Thesis, School of Engineering, Air Force Institute of Technology, Wright-Patterson AFB, Ohio, 1980.

5. Hasegawa, Capt Glenn K. Former Chief, Deep Space Surveillance, NORAD Cheyenne Mountain Complex, Colorado. Personal interview.

6. Infrared Handbook. Washington, D.C. Environmental Research Institute of Michigan, 1978.

7. Lange, James J. Class Notes Distributed in PH 6.21, Electro-optical Space Systems Technology. School of Engineering, Air Force Institute of Technology, Wright-Patterson AFB, Ohio, April, 1983.

8. Pensa, A. F. Deep Space Radar Surveillance: A Network Approach. Project Report STK-125. Lexington, Massachusetts: Lincoln Laboratory/Massachusetts Institute of Technology, 30 July 1982.

9. Russell, David M. "NORAD Adds Radar, Optics to Increase Space Defense," Defense Electronics 14:82-86 (July 1982).

10. Shannon, Robert E. Systems Simulation: The Art and Science. Englewood Cliffs, N.J.: Prentice-Hall, Inc., 1975.

11. "SPACECOM Seeks ASAT Laser," Aviation Week and Space Technology, 118:18-19 (21 March 1983).

12. "Space Surveillance Deemed Inadequate," Aviation Week and Space Technology, 112:249-255 (16 June 1980).

13. Sridrahan, S. and W. Sinieu. Deep Space Group, MIT Lincoln Labatory. Telephone interviews 27 and 29 July 1983.

14. Stark, Peter A. Introduction to Numerical Methods. New York: The Macmillan Company, 1970.

15. Vandergraft, James S. Introduction to Numerical Computations. New York: The Academic Press, 1978.

16. Whitcomb, David W. Personal Correspondence. The Aerospace Corporation, Los Angeles, CA, 4 August 1983.

Appendix

Program Listing

Program ASAT was written to be run interactively, and appears as such. However, should a user care to run in batch (card deck) mode, a few simple changes would complete the conversion. First of all, there would be no need for the "OPEN" statement to create file "OUTLST." Next, the input statements would be replaced by a "READ" statement to read the input parameters from data cards at the end of the card deck. Finally, all the "WRITE" statements would be changed to write to the standard output device ("*") instead of file 50. On the following pages appears the program listing for the interactive version used by the author.

```
      PROGRAM ASAT
******
******
******
************************************************************************
******
******
******PROGRAM ASAT WAS PRODUCED AS PARTIAL FULFILLMENT OF  THE
******REQUIREMENTS FOR THE DEGREE OF MASTER OF SCIENCE IN SPACE
******OPERATIONS, AIR FORCE INSTITUTE OF TECHNOLOGY.
******
******          PROGRAMMER:CAPT RICHARD C. BARCLAY
******                      AFIT CLASS GSO-83D
******
******
******      THESIS ADVISOR:LT COL MARK M. MEKARU
******                      ASST PROF OF OPS RESEARCH
******                      AFIT,WPAFB,OH
******                      AUTOVON 785-2549
******
******THIS PROGRAM IS INTENDED TO BE USED AS A TOOL IN A FIRST CUT
******EVALUATION OF A DEEP SPACE ANTI-SATELLITE SYSTEM. IT USES MONTE
******CARLO ERROR GENERATION TO EXAMINE THE EFFECTS OF INTERCEPTOR VEHI-
******CLE GUIDANCE ERRORS, TARGET TRACKING ERRORS, AND THEIR IMPACT ON
******ASAT ACQUISITION SENSOR AND MANEUVER CAPABILITIES.  THE USER
******INPUTS AN INITIAL POSITION, FINAL POSITION, AND TIME OF FLIGHT
******FROM WHICH A NOMINAL INTERCEPT TRAJECTORY IS COMPUTED AND USED
******AS A BASELINE FOR COMPARISON IN THE ERROR GENERATION PORTION OF
******THE PROGRAM.  FOR THAT ERROR GENERATION PORTION, THE USER INPUTS
******ERROR CHARACTERISTICS OF BOTH THE INTERCEPTOR VEHICLE AND THE
******TARGET.  THOSE ARE USED TO 'SCALE' THE COMPONENTS OF INTERCEPT
******VEHICLE ERROR IN POSITION AND VELOCITY, AS IT BEGINS 'FREE
******FLIGHT', AND THE TARGET POSITION AT INTERCEPT.  ADDITIONALLY,
******SINCE THESE ERRORS ARE MOST EASILY CHARACTERIZED IN THE 'RADIAL-
******TANGENTIAL-NORMAL(R-T-N)' COORDINATE SYSTEM, THE USER ALSO MUST
******INPUT THE TARGET VELOCITY VECTOR AT INTERCEPT TO FACILITATE
```

```
******THE TRANSFORMATION FROM R-T-N TO GEOCENTRIC-EQUATORIAL SYSTEM.
**********************************************************************
******
******
******
      REAL R1I,R1J,R1K,R2I,R2J,R2K,TOF,V1I,V1J,V1K,V2I,V2J,V2K,
     +RNNS,V1INEW,V1JNEW,V1KNEW,R2INEW,R2JNEW,R2KNEW,V2INEW,
     +V2JNEW,V2KNEW,R2NEWM,V2NEWM,DELR,DELV,R1M,R2M,V1M,V2M
     +,DELR2I,DELR2J,DELR2K,DELV2I,DELV2J,DELV2K,DLRTOT,DLRAVG
     +,COMPRI,COMPRJ,COMPRK,COMPVI,COMPVJ,COMPVK,R1INEW,R1JNEW,R1KNEW,
     +SCALPR,SCALPT,SCALRN,SCALVR,SCALVT,SCALVN
     +,V1IT,V1JT,V1KT,SCALTR,SCALTT,SCALTN,COMPTI,COMPTJ,COMPTK,
     +DELV1T,DELV2T,DELV3T,DELV4T,DELV1,DELV2,DELV3,DELV4,DVA1,
     +DVA2,DVA3,DVA4,R2IT,R2JT,R2KT,V2IT,V2JT,V2KT
     +,DLPSQT,DELV0,DELVOT,DVA0,VAR,STDEV,DVOTSQ,DVVAR,DVSD
      INTEGER N
      OPEN(50,FILE='OUTLST')
******
******
**********************************************************************
******AT THIS POINT THE INPUT DATA IS READ IN THE FOLLOWING ORDER:
******(1-3) INITIAL POSITION(I,J,K COMPONENTS,RESPECTIVELY);
******(4-6) FINAL POSITION(I,J,K COMPONENTS, RESPECTIVELY);
******( 7 ) TIME OF FLIGHT
******(8-10)SCALE FACTORS FOR POSITION ERROR OF INTERCEPTOR(R,T,N)
******(11-13)SCALE FACTORS FOR INTERCEPTOR VELOCITY ERROR(R,T,N)
******(14-16)SCALE FACTORS FOR TARGET TRACKING ERRORS(R,T,N)
******(17-19)TARGET VELOCITY(I,J,K)
******ALL ENTRIES IN GEOCENTRIC CANONICAL UNITS*******************
**********************************************************************
******
******
      R1I=.84803
      R1J=0
      R1K=.58283
      R2I=1.15
```

```
          R2J=6.5222
          P2K=0
          TOF=17.857993
          SCALRP=1.32E-4
          SCALRT=1.32E-4
          SCALRN=1.32E-4
          SCALVR=1.32E-4
          SCALVT=1.32E-4
          SCALVN=1.32E-4
          V2IT=-.38268
          V2JT=.06748
          V2KT=0
          SCALTR=3.1357E-4
          SCALTT=3.1357E-3
          SCALTN=3.1357E-4
          DLPTOT=0
          DLRAVG=0
          DLRSQT=0
          DV0TSQ=0
          DELVPT=0
          DELV1T=0
          DELV2T=0
          DELV3T=0
          DELV4T=0
          DVA1=0
          DVA0=0
          DVA2=0
          DVA3=0
          DVA4=0
******
******
**************************************************************
******THIS CALL ESTABLISHES THE NOMINAL INTERCEPT*************
**************************************************************
******
******
```

```
      CALL INTCPT(R1I,R1J,R1K,R2I,R2J,R2K,TOF,V1I,V1J,V1K,V2I,V2J,V2K,
     +R1M,R2M,V1M,V2M)
      WRITE(50,170)
  170 FORMAT(//,' RESULTS OF RANDOM ERRORS:',//,
     +' ATTEMPT#',2X,'MISS DISTANCE(DU)')
******
******
***************************************************************
******THIS DO-LOOP RUNS 500 INTERCEPTS WITH RANDOMLY GENERATED
******ERRORS AND COMPUTES A MISS DISTANCE FOR EACH RUN
***************************************************************
******
******
      DO 80 N=1,500,1
         CALL RNDMGN(SCALRR,SCALRT,SCALRN,R1I,R1J,R1K,V1I,V1J,V1K,
     +COMPRI,COMPRJ,COMPRK)
         R1INEW=R1I+COMPRI
         R1JNEW=R1J+COMPRJ
         R1KNEW=R1K+COMPRK
         CALL RNDMGN(SCALVR,SCALVT,SCALVN,R1I,R1J,R1K,V1I,V1J,V1K,
     +COMPVI,COMPVJ,COMPVK)
         V1INEW=V1I+COMPVI
         V1JNEW=V1J+COMPVJ
         V1KNEW=V1K+COMPVK
         CALL RNDMGN(SCALTR,SCALTT,SCALTN,R2I,R2J,R2K,V2IT,V2JT,V2KT,
     +COMPTI,COMPTJ,COMPTK)
         R2IT=R2I+COMPTI
         R2JT=R2J+COMPTJ
         R2KT=R2K+COMPTK
         CALL KEPLER(R1INEW,R1JNEW,R1KNEW,V1INEW,V1JNEW,V1KNEW,TOF,
     +R2INEW,R2JNEW,R2KNEW,V2INEW,V2JNEW,V2KNEW,R2NEWM,V2NEWM)
         DELR2I=R2IT-R2INEW
         DELR2J=R2JT-R2JNEW
         DELR2K=R2KT-R2KNEW
         DELR=SQRT(DELR2I**2+DELR2J**2+DELR2K**2)
         DELV0=(V2NEWM*DELR)/3.9196227E-2
      DELV1=(V2NEWM*DELR)/7.8392453E-2
      DELV2=(V2NEWM*DELR)/1.5678491E-1
      DELV3=(V2NEWM*DELR)/.2351774
      DELV4=(V2NEWM*DELR)/.3135698
      WRITE(50,160)N,DELR
  160 FORMAT(4X,I3,5X,F12.8)
      DLRTOT=DLRTOT+DELR
      DLRSQT=DLRSQT+DELR**2
      DV0TSQ=DV0TSQ+DELV0**2
      DELV0T=DELV0T+DELV0
      DELV1T=DELV1T+DELV1
      DELV2T=DELV2T+DELV2
      DELV3T=DELV3T+DELV3
      DELV4T=DELV4T+DELV4
   80 CONTINUE
******
******
*****************************************************************
******THE FOLLOWING STEPS COMPUTE MEAN, VARIANCE, AND STANDARD
******DEVIATION OF MISS DISTANCE AND SELECTED DELTA V FOR ALL
******THE INTERCEPTS RUN IN THE ERROR MODE
*****************************************************************
******
******
      DLRAVG=(DLRTOT/500)*6378.165
      VAR=((DLRSQT-(DLRTOT**2/500))/499)*6378.165
      STDEV=SQRT(VAR)
      DVVAR=((DV0TSQ-(DELV0T**2/500))/499)*7.905376
      DVSD=SQRT(DVVAR)
      DVA0=(DELV0T/500)*7.905376
      DVA1=(DELV1T/500)*7.905376
      DVA2=(DELV2T/500)*7.905376
      DVA3=(DELV3T/500)*7.905376
      DVA4=(DELV4T/500)*7.905376
      WRITE(50,130)DLRAVG,STDEV,VAR,DVA0,DVSD,DVVAR,DVA1,DVA2,DVA3,DVA4
  130 FORMAT(///,' MEAN MISS DISTANCE(500 INTERCEPTS)=',F9.5,' KM',/,
     +5X,'WITH A STD. DEV. OF ',F14.8,' AND VAR. OF ',F14.8,/,
     +' MEAN DELTA VEE FOR ACQUISITION AT 250KM= ',F9.5,' KM/SEC',/,
     +5X,'STD. DEV.= ',F14.8,4X,'VAR.= ',F14.8,/,
     +' MEAN DELTA VEE FOR ACQUISITION AT 500KM= ',F9.5,' KM/SEC',/,
     +' MEAN DELTA VEE FOR ACQUISITION AT 1000KM= ',F9.5,' KM/SEC',/,
     +' MEAN DELTA VEE FOR ACQUISITION AT 1500KM= ',F9.5,' KM/SEC',/,
     +' MEAN DELTA VEE FOR ACQUISITION AT 2000KM= ',F9.5,' KM/SEC')
      END


******************************************************************
******THIS SUBROUTINE GENERATES ERRORS USING THE INPUT ERROR
******CHARACTERISTICS('SCALE FACTORS') IN R-T-N SYSTEM AND
******OUTPUTS ERROR COMPONENTS IN I-J-K SYSTEM
******************************************************************
******
******
      SUBROUTINE RNDMGN(SCALER,SCALET,SCALEN,RI,RJ,RK,VI,VJ,VK,
     +COMPOI,COMPOJ,COMPOK)
      REAL RN(12),RNN(3),RNNS(3),RNTOT,SCALE(3),COMPOI,COMPOJ,COMPOK,
     +SCALER,SCALET,SCALEN,RI,RJ,RK,VI,VJ,VK,RM,TM,NM,R(3),T(3),N(3)
      INTEGER M,P
      SCALE(1)=SCALER
      SCALE(2)=SCALET
      SCALE(3)=SCALEN
      DO 90 P=1,3,1
      RNTOT=0
      DO 70 M=1,12,1
         RN(M)=RANF()
         RNTOT=RNTOT+RN(M)
   70 CONTINUE
      RNN(P)=RNTOT-6
      RNNS(P)=SCALE(P)*RNN(P)
   90 CONTINUE
```

```
      RM=SQRT(RI**2+RJ**2+RK**2)
      R(1)=(RI/RM)*RNNS(1)
      R(2)=(RJ/RM)*RNNS(1)
      R(3)=(RK/RM)*RNNS(1)
      N(1)=RJ*VK-RK*VJ
      N(2)=VI*RK-RI*VK
      N(3)=RI*VJ-RJ*VI
      NM=SQRT(N(1)**2+N(2)**2+N(3)**2)
      N(1)=(N(1)/NM)*RNNS(3)
      N(2)=(N(2)/NM)*RNNS(3)
      N(3)=(N(3)/NM)*RNNS(3)
      T(1)=RK*N(2)-RJ*N(3)
      T(2)=RI*N(3)-RK*N(1)
      T(3)=RJ*N(1)-RI*N(2)
      TM=SQRT(T(1)**2+T(2)**2+T(3)**2)
      T(1)=(T(1)/TM)*RNNS(2)
      T(2)=(T(2)/TM)*RNNS(2)
      T(3)=(T(3)/TM)*RNNS(2)
      COMPOI=R(1)+T(1)+N(1)
      COMPOJ=R(2)+T(2)+N(2)
      COMPOK=R(3)+T(3)+N(3)
      END

      SUBROUTINE INTCPT(R1I,R1J,R1K,R2I,R2J,R2K,TOF,V1I,V1J,V1K,
     +V2I,V2J,V2K,RONEM,RTWOM,VONEM,VTWOM)
******
******
*****************************************************************
******THIS SUBROUTINE USES THE INTERCEPTOR'S INITIAL POSITION
******VECTOR(R1/RONE),FINAL POSITION VECTOR(R2/RTWO), AND TIME
******OF FLIGHT BETWEEN THE TWO TO COMPUTE THE VELOCITY
******VECTORS(V1/VONE,V2/VTWO) AT EACH POSITION.  IT
******ASSUMES THAT THE VEHICLE TAKES THE 'SHORT WAY' TRAJEC-
******TORY (I.E. THE ANGLE BETWEEN RONE AND RTWO IS LESS THAN
******180 DEGREES).
*****************************************************************
```

```
******
******
      REAL RONE(3),RTWO(3),TOF,DELNU,RONEM,RTWOM,RDOT,A,ZUPR,ZLWR,
     +ZMDPT,S,C,Y,X,TIM,F,G,GDOT,VONE(3),VTWO(3),VONEM,VTWOM
     +,R1I,R1J,R1K,R2I,R2J,R2K,V1I,V1J,V1K,V2I,V2J,V2K
      INTEGER I,J
      PARAMETER(PI=3.14159265359)
      RONE(1)=R1I
      RONE(2)=R1J
      RONE(3)=R1K
      RTWO(1)=R2I
      RTWO(2)=R2J
      RTWO(3)=R2K
      RONEM=SQRT(RONE(1)**2+RONE(2)**2+RONE(3)**2)
      RTWOM=SQRT(RTWO(1)**2+RTWO(2)**2+RTWO(3)**2)
      WRITE(50,110)RONE(1),RONE(2),RONE(3),RONEM,RTWO(1),RTWO(2),
     +RTWO(3),RTWOM,TOF
  110 FORMAT(//,' NOMINAL INTERCEPT INPUTS:',/,' R1=',F12.8,'I+',F12.8,
     +'J+',F12.8,'K',/,' R1(MAGNITUDE)=',F12.8,/,' R2=',F12.8,'I+',
     +F12.8,'J+',F12.8,'K',/,' R2(MAGNITUDE)=',F12.8,/,
     +' TIME OF FLIGHT(TU)=',F12.8)
      RDOT=RONE(1)*RTWO(1)+RONE(2)*RTWO(2)+RONE(3)*RTWO(3)
      DELNU=ACOS(RDOT/(RONEM*RTWOM))
      A=(SQRT(RONEM*RTWOM)*SIN(DELNU))/(SQRT(1-COS(DELNU)))
      ZUPR=(2*PI)**2
      ZLWR=0
******
******
*******************************************************************
******THIS "DO LOOP" USES THE BISECTION TECHNIQUE OF NUMER-
******ICAL ITERATION WITH UNIVERSAL VARIABLE FORMULATION AS
******PRESENTED IN "FUNDAMENTALS OF ASTRODYNAMICS" BY BATE,
******MUELLER,AND WHITE TO ENABLE COMPUTATION OF THE DESIRED
******VELOCITY VECTORS
******************************************************************
******
```

```
******
      DO 10  I=1,30,1
         ZMDPT=0.5*(ZUPR+ZLWR)
         S=(SQRT(ZMDPT)-SIN(SQRT(ZMDPT)))/SQRT(ZMDPT**3)
         C=(1-COS(SQRT(ZMDPT)))/ZMDPT
         Y=RONEM+RTWOM-(A*(1-(ZMDPT*S)))/SQRT(C)
         X=SQRT(Y/C)
         TIM=((X**3)*S)+(A*SQRT(Y))
         IF(TIM.GT.TOF) THEN
            ZUPR=ZMDPT
           ELSE
            ZLWR=ZMDPT
         ENDIF
   10 CONTINUE
      F=1-(Y/RONEM)
      G=A*SQRT(Y)
      GDOT=1-(Y/RTWOM)
      DO 20  J=1,3,1
         VONE(J)=(RTWO(J)-F*RONE(J))/G
         VTWO(J)=(GDOT*RTWO(J)-RONE(J))/G
   20 CONTINUE
      VONEM=SQRT(VONE(1)**2+VONE(2)**2+VONE(3)**2)
      VTWOM=SQRT(VTWO(1)**2+VTWO(2)**2+VTWO(3)**2)
      WRITE(50,120)
  120 FORMAT(//,' NOMINAL INTERCEPT VELOCITY VECTORS ARE:',/)
      WRITE(50,130) VONE(1),VONE(2),VONE(3),VONEM,VTWO(1),VTWO(2),VTWO(3)
     +,VTWOM
  130 FORMAT(//,' THE I COMPONENT OF V1 IS',F11.8,/,
     +' THE J COMPONENT OF V1 IS',F11.8,/,' THE K COMPONENT OF V1 IS',
     +F11.8,/,' THE MAGNITUDE OF V1 IS',F11.8,///,
     +' THE I COMPONENT OF V2 IS',F11.8,/,' THE J COMPONENT OF V2 IS',
     +F11.8,/,' THE K COMPONENT OF V2 IS',F11.8,/,
     +' THE MAGNITUDE OF V2 IS',F11.8)
      V1I=VONE(1)
      V1J=VONE(2)
      V1K=VONE(3)
      V2I=VTWO(1)
      V2J=VTWO(2)
      V2K=VTWO(3)
      END

      SUBROUTINE KEPLER(R1I,R1J,R1K,V1I,V1J,V1K,TOF,R2I,R2J,R2K,V2I,
******
******
**************************************************************
******THIS SUBROUTINE USES THE 'KEPLER' ALGORITHM AS PRESENTED IN
******'FUNDAMENTALS OF ASTRODYNAMICS' BY BATE, MUELLER, AND WHITE.
******USING THE RECOMPUTED INITIAL POSITION AND VELOCITY VECTORS AND
******THE GIVEN TIME OF FLIGHT, THIS SUBROUTINE RECOMPUTES THE
******INTERCEPT TRAJECTORY AND OUTPUTS A NEW POSITION AND VELOCITY
******VECTOR AT THE GIVEN TIME OF FLIGHT.
*******************************************************************
******
******
     +V2J,V2K,RTWOM,VTWOM)
      REAL RONE(3),RTWO(3),VONE(3),VTWO(3),RONEM,RTWOM,VONEM,VTWOM,TOF,
     +RDOTV,ALPH,XN,ZN,CN,SN,TN,DTDX,F,FDOT,G,GDOT,CHECKR,SME
     +,R1I,R1J,R1K,R2I,R2J,R2K,V1I,V1J,V1K,V2I,V2J,V2K
      INTEGER K,L
      RONE(1)=R1I
      RONE(2)=R1J
      RONE(3)=R1K
      VONE(1)=V1I
      VONE(2)=V1J
      VONE(3)=V1K
      RONEM=SQRT(RONE(1)**2+RONE(2)**2+RONE(3)**2)
      VONEM=SQRT(VONE(1)**2+VONE(2)**2+VONE(3)**2)
      RDOTV=RONE(1)*VONE(1)+RONE(2)*VONE(2)+RONE(3)*VONE(3)
      ALPH=2/RONEM-VONEM**2
      SME=-ALPH/2
      XN=TOF*ALPH
```

```
40 ZN=ALPH*(XN**2)
   IF (ZN.NE.0) THEN
      CN=(1-COS(SQRT(ZN)))/ZN
      SN=(SQRT(ZN)-SIN(SQRT(ZN)))/SQRT(ZN**3)
   ELSE
      CN=0.5
      SN=0.16666667
   ENDIF
   TN=RDOTV*XN**2*CN+(1-ALPH*RONEM)*XN**3*SN+RONEM*XN
   IF(ABS(TOF-TN).GT.0.5E-6) THEN
      DTDX=XN**2*CN+RDOTV*XN*(1-ZN*SN)+RONEM*(1-ZN*CN)
      XN=XN+(TOF-TN)/DTDX
      GO TO 40
   ENDIF
   F=1-(XN**2*CN)/RONEM
   G=TOF-XN**3*SN
   DO 50 K=1,3,1
      RTWO(K)=F*RONE(K)+G*VONE(K)
50 CONTINUE
   RTWOM=SQRT(RTWO(1)**2+RTWO(2)**2+RTWO(3)**2)
   FDOT=(1/(RONEM*RTWOM))*XN*(ZN*SN-1)
   GDOT=1-(XN**2*CN)/RTWOM
   DO 60 L=1,3,1
      VTWO(L)=FDOT*RONE(L)+GDOT*VONE(L)
60 CONTINUE
   RTWOM=SQRT(RTWO(1)**2+RTWO(2)**2+RTWO(3)**2)
   VTWOM=SQRT(VTWO(1)**2+VTWO(2)**2+VTWO(3)**2)
   CHECKR=F*GDOT-FDOT*G
   R2I=RTWO(1)
   R2J=RTWO(2)
   R2K=RTWO(3)
   V2I=VTWO(1)
   V2J=VTWO(2)
   V2K=VTWO(3)
   END
```

VITA

Captain Richard C. Barclay was born on 8 June 1952 in East Cleveland, Ohio. After graduating from North High School in Eastlake, Ohio, he accepted an appointment to the Air Force Academy. He graduated from the Academy in 1974, with a Bachelor of Science degree in Astronautical Engineering. After earning his pilot wings in Undergraduate Pilot Training at Columbus AFB, Mississippi, Captain Barclay flew WC-130 aircraft with the 54th Weather Reconnaissance Squadron, Andersen AFB, Guam. Captain Barclay has also been an Aircraft Commander with the 21st Tactical Airlift Squadron, Clark AB, Philippines, an instructor pilot with the 4953rd Test Squadron, Wright-Patterson AFB, Ohio, and an Air Staff Training Officer at Headquarters, USAF prior to his assignment to the Air Force Institute of Technology in June, 1982.

Permanent Address: 29005 Forest Grove
Willowick, OH 44094

UNCLASSIFIED
SECURITY CLASSIFICATION OF THIS PAGE

REPORT DOCUMENTATION PAGE

1a. REPORT SECURITY CLASSIFICATION JNCLASSIFIED

1b. RESTRICTIVE MARKINGS

2a. SECURITY CLASSIFICATION AUTHORITY

2b. DECLASSIFICATION/DOWNGRADING SCHEDULE

3. DISTRIBUTION/AVAILABILITY OF REPORT
Approved for public release;
distribution unlimited

4. PERFORMING ORGANIZATION REPORT NUMBER(S) AFIT/GSO/OS/83-D1

5. MONITORING ORGANIZATION REPORT NUMBER(S)

6a. NAME OF PERFORMING ORGANIZATION School of Engineering

6b. OFFICE SYMBOL *(If applicable)* AFIT/EN

7a. NAME OF MONITORING ORGANIZATION

6c. ADDRESS *(City, State and ZIP Code)*
Air Force Institute of Technology
Wright-Patterson AFB, Ohio 45433

7b. ADDRESS *(City, State and ZIP Code)*

8a. NAME OF FUNDING/SPONSORING ORGANIZATION HQ SPACECOM

8b. OFFICE SYMBOL *(If applicable)* DOZ

9. PROCUREMENT INSTRUMENT IDENTIFICATION NUMBER

8c. ADDRESS *(City, State and ZIP Code)*
HQ SPACECOM/DOZ
Stop 7
Peterson AFB, Colorado 80914

10. SOURCE OF FUNDING NOS.

PROGRAM ELEMENT NO.	PROJECT NO.	TASK NO.	WORK UNIT NO.

11. TITLE *(Include Security Classification)* See Box 19

12. PERSONAL AUTHOR(S) Richard C. Barclay, B.S.A.E., Capt., USAF

3a. TYPE OF REPORT MS Thesis

13b. TIME COVERED FROM ________ TO ________

14. DATE OF REPORT *(Yr., Mo., Day)* 1983 December

15. PAGE COUNT 89

16. SUPPLEMENTARY NOTATION

Approved for public release: IAW AFR 190-17.
Lynn Wolaver 7 May 84
LYNN E. WOLAVER
Dean for Research and Professional Development
Air Force Institute of Technology (ATC)
Wright-Patterson AFB OH 45433

17. COSATI CODES

FIELD	GROUP	SUB. GR.

18. SUBJECT TERMS *(Continue on reverse if necessary and identify by block number)*
ASAT, Deep Space, Deep Space Tracking
Error Assignments

19. ABSTRACT *(Continue on reverse if necessary and identify by block number)*

Title: A COMPUTER MODEL FOR EVALUATION OF LAUNCH VEHICLE AND TARGET TRACKING ERROR ASSIGNMENTS FOR DIRECT ASCENT, DEEP SPACE ASAT SYSTEMS

Thesis Chairman: Mark Mekaru, Lt Col, USAF

An unclassified computer model was developed for first order evaluation of deep space Anti-satellite (ASAT) targeting error assignments. Two independent error sources are modeled. With deep space tracking accuracies on the order of kilometers, there is uncertainty in the exact target position. Errors introduced by the launch vehicle guidance system result in uncertainty in the exact position of the ASAT itself. Once the target is acquired by the ASAT sensor subsystem, the maneuver subsystem must then have the capability to make the necessary trajectory corrections to prevent a "miss."

The model assumes a direct ascent vehicle for which the user selects a trajectory

20. DISTRIBUTION/AVAILABILITY OF ABSTRACT
ICLASSIFIED/UNLIMITED ☒ SAME AS RPT. ☐ DTIC USERS ☐

21. ABSTRACT SECURITY CLASSIFICATION UNCLASSIFIED

22a. NAME OF RESPONSIBLE INDIVIDUAL Mark Mekaru, Lt Col, USAF

22b. TELEPHONE NUMBER *(Include Area Code)* (513) 255-2549

22c. OFFICE SYMBOL AFIT/ENS

DD FORM 1473, 83 APR EDITION OF 1 JAN 73 IS OBSOLETE.

SECURITY CLASSIFICATION OF THIS PAGE

by choosing the burnout and intercept position vectors, and a time of flight between them. Monte Carlo simulation is used to generate errors in burnout position and velocity, and intercept position from trivariate normal distributions scaled to user input standard deviations. This is repeated for 500 iterations, from which a mean miss distance and delta V required for trajectory correction can be determined, and used for further analysis.

Suggested applications are presented to show how the model results can be used as a measure of system performance for initial system tradeoff studies. Validation/verification and recommendations for further use are also provided. A program listing is included as an appendix.